Universitat de Girona

ANALYSIS AND OPTIMIZATION OF COMPOSITE STRINGERS

Pere BADALLÓ i CAÑELLAS

Dipòsit legal: Gi. 1387-2015
http://hdl.handle.net/10803/323087

Universitat de Girona

DOCTORAL THESIS

ANALYSIS AND OPTIMIZATION OF COMPOSITE STRINGERS

Pere Badalló i Cañellas

2015

Universitat de Girona

DOCTORAL THESIS

ANALYSIS AND OPTIMIZATION OF COMPOSITE STRINGERS

Pere Badalló i Cañellas

2015

Doctorat en Tecnologia

Advisor: Daniel Trias i Mansilla

THESIS SUBMITTED FOR THE DEGREE OF DOCTOR BY UNIVERSITAT DE GIRONA

Al meu avi Àngel,

"... encara ens resta l'esperança
de que algun dia ens trobrem al Cel."

Josep M. de Sagarra

Agraïments - Acknowledgements

Primerament voldria agrair al meu director Dr. Dani Trias i Mansilla l'oportunitat de poder dur a terme aquesta tesi sota la seva supervisió. També per la seva paciència amb el meu anglès.

I would like to thank Dr. Esben Lindgaard for his support and his time during my research stay at Aalborg Universitet. I would also like to acknowledge all the people from the Department of Mechanical and Manufacturing Engineering of Aalborg Universitet, especially to my office mates Georgios Martakos and Brian Bak. My time in Aalborg was awesome.

Evidentment no puc oblidar a tota la gent que ha passat pel grup de recerca AMADE de la Universitat de Girona. Després d'aquests anys, hem passat moments estel·lars tot explicant-nos les penes o fer-nos un fart de riure. Realment sense vosaltres, que us heu vist obligats a compartir amb mi tantes hores, el meu camí hagués estat molt més dur. Us trobaré a faltar. Gràcies!

Als meus companys de viatge diari: l'Albert Turon i la Marta Baena. Ells han fet que els quilòmetres que separen casa meva de la universitat fossin molt més amens. Riures, debats, històries, anècdotes i un llarg etcètera. Realment ha estat un autèntic plaer poder compartir tantes hores en un espai tan reduït com és un cotxe. Gràcies per escurçar la distància!

A tots els membres de l'Agrupament Escolta Montnegre (infants, joves i caps) i als Amics Escoltes del Montnegre que m'han permès tenir moments únics que mai hagués pogut viure de no ser per vosaltres. He sentit, sento i sentiré un #orgullMontnegre inimaginable! La meva tesi té, de ben segur, una part vostra. Sempre a punt!

A la gent de la Colla de Geganters i Grallers de Calella que tantes bones estones m'ha fet passar. Continuarem mirant amunt!

Als bons amics de la colla (i els que m'he trobat pel camí arreu de Catalunya). Que, tot i no saber molt bé el que feia, m'heu donat ànims sempre. Després de tants anys continueu aquí. Especialment a en Marc i la Marina, pels anys i anys d'amistat i recolzament. Tots plegats, si voleu saber què he fet durant aquests anys, només heu de llegir-ho!

I, sobretot, a la meva estimada família. A les meves dues àvies Maria i Dolors, que sempre em teniu present i esteu pensant en el nét que va amunt i avall. Al meu germà Àngel, que sense dir massa res, sempre hi ets i ho sé. Sempre a la nostra manera. Als meus pares Imma i Àngel, que m'han ensenyat que amb amor les coses difícils es fan fàcils i les quasi impossibles són possibles. No us ho podré agrair mai prou. Gràcies, gràcies i gràcies!

The present work has been funded by Universitat de Girona under research grant BR2011/02.

This Ph.D. thesis has been prepared as a compendium of papers, according to the regulations of Universitat de Girona (*Normativa d'ordenació dels ensenyaments universitaris de doctorat de la Universitat de Girona, aprovada pel Consell de Govern en al sessió 3/12, de 26 d'abril de 2012, i modificada pel Consell de Govern en la sessió 5/2013, de 25 de setembre de 2013*). This thesis includes three original papers: One paper that has already been published in a peer-reviewed journal, and another two have already been submitted.

The complete references of the papers comprising this thesis, the impact factors, quartile, and category of the journals are:

- P. Badalló, D. Trias, L. Marín, J. A. Mayugo. *A comparative study of genetic algorithms for the multi-objective optimization of composite stringers under compression loads*. Composites Part B: Engineering 2013; 47(0):130-136.

  ISSN: 1359-8368

  doi: 10.1016/j.compositesb.2012.10.037

  Impact factor: 2.602; Journal 7 of 87; 1st quartile; Category: Engineering, Multidisciplinary.

- P. Badalló, D. Trias, L. Marín, Ll. Ripoll. *Virtual test of different types of composite stringer run-outs under tensile load*. Submitted to Engineering Failure Analysis at March 2015.

  Impact factor: 1.130; Journal 8 of 33; 1st quartile; Category: Materials Science, Characterization & Testing.

- P. Badalló, D. Trias, E. Lindgaard. *Damage tolerance optimization of composite stringer run-out under tensile load*. Submitted to Composite Structures at March 2015.

  Impact factor: 3.120; Journal 2 of 24; 1st quartile; Category: Materials Science, Composites.

The three papers have been published in (or submitted to) journals with impact factors within the first quartile, according to the 2013 Journal Citation Reports.

Girona, May 2015

Pere Badalló i Cañellas
Universitat de Girona

To whom it might concern,

Dr. Daniel Trias i Mansilla, Professor at Universitat de Girona of Departament d'Enginyeria Mecànica i de la Construcció Industrial

CERTIFIES that the study entitled *Analysis and optimization of composite stringers* has been carried out under his supervision by Pere Badalló i Cañellas to apply for the doctoral degree with International Mention.

Girona, May 2015

Dr. Daniel Trias i Mansilla
Universitat de Girona

List of Figures

1.1 Stiffened panels. 11
1.2 Example of stringer run-out. 12
1.3 Scheme of time reduction using virtual testing. 13
1.4 Two operators of GAs. 14

2.1 Stringer section and schematic representation of the test. 23
2.2 Benchmark problem. 24
2.3 P_{cr} vs. L_{B}. 25
2.4 P_{cr} vs. L_{S}. 26
2.5 P_{cr} vs. L_{B} and L_{S}. 27
2.6 Evolution of the optimums. 32

3.1 Schematic representation and FE model of the test. 39
3.2 Design variables and types of stringer run-outs. 40
3.3 Stiffness vs. Force. 43
3.4 Force vs. Displacement. 44
3.5 Normalized $\mathcal{G}/\mathcal{G}_C$ vs. crack length. 45
3.6 Displacements of the panel in Y-axis before failure. 46
3.7 Evolution of shear mode ratio B in the crack tip of T2. 47

4.1 Schematic representation of the test and the initial design variables. 53
4.2 Details of the finite element model. 55
4.3 Initial data sampling. 58
4.4 Exemple of smoothed RBF. 59
4.5 B vs. d when $\beta = 0°$. 64

List of Tables

2.1 AS4/8552 properties. 24
2.2 Summary of obtained results. 30
2.3 Statistics of the results. 31
2.4 Mann-Whitney test results. 31

3.1 FM-300K properties. 41
3.2 Comparison with experimental results. 44
3.3 Cohesive element stresses in the proximity of the crack tip. 47

4.1 AS4/8552 and FM-300K properties. 54
4.2 Results of comparative study of the element type. 55
4.3 Results of the ANOVA test. 57
4.4 Comparative error of RBF. 62
4.5 Results of LS of the RBF. 62
4.6 Interval optimums. 63

Contents

Abstract **3**

1 Introduction and objectives **9**
1.1 Introduction 11
1.2 Stiffened panels 11
1.3 Virtual tests 12
1.4 Genetic algorithms 13
1.5 Metamodeling 14
1.6 Objectives 15

2 A comparative study of genetic algorithms **17**
2.1 Introduction 20
2.2 Benchmark problem 22
2.2.1 Specimen 22
2.2.2 Virtual test 23
2.2.3 Preliminary study 23
2.3 Multi-objective optimization 27
2.4 Results and Discussion 29
2.5 Conclusion 32

3 Virtual test of different types of composite stringer run-outs **35**
3.1 Introduction 38
3.2 Virtual test 38
3.2.1 Specimen and test 38
3.2.2 Simulation of panel-stringer debonding 41
3.3 Results and Discussion 41
3.3.1 Damage 41
3.3.2 Displacements 45

3.3.3 Fracture modes analysis 46
3.3.4 Stress analysis 47
3.4 Conclusions 48

4 Damage tolerance optimization of composite stringer run-out 49
4.1 Introduction 52
4.2 Virtual test 53
4.2.1 Specimen and test 53
4.2.2 Virtual Crack Closure Technique 56
4.3 Optimization 56
4.3.1 Design variables 56
4.3.2 Optimization problem 57
4.3.3 Data sampling 58
4.3.4 Radial Basis Functions 58
4.4 Results and Discussion 61
4.5 Conclusion 64

5 Conclusions 67

Bibliography 72

Appendices 81

A Published paper 81

Abstract

The use of the stiffened panels in the aircraft/aeronautical industry has been growing in the last decades. Thanks to the stringers added on the panels, an increase of the stiffness without a substantial increment of the weight can be achieved. The diversity of the stringer typology and the widespread use have generated a field of study with a significant presence in the scientific literature. On the other hand, the exponential growth in the use of composite materials in the last years has had a strong influence in these structural components and in the industry in general. Composite materials are compounded of two constitutive materials (named matrix and reinforcement). This union offers new improved properties completely different from the two separated materials. In consequence, with this new material unknown characteristics appear, for example new failure mechanisms, producing high complexity when simulation, analysis and testing are performed. For this reason, thanks to the increment in the power of the computers, the use of virtual tests with finite element method has become crucial in the simulation of the components with high structural responsibility. In the same way, the general spread of computational resources has made possible the use of optimization methods in the design process of stiffened panels. Optimization methods are able to find the best design according to some criteria, by modifying different parameters: geometric parameters, boundary conditions or material definition, for example. Some optimization methods are based on the infinitesimal calculus and imply the numerical computation of derivatives (gradients). Conversely, the so-called heuristic optimization methods try to reproduce processes seen in nature.

Genetic Algorithms (GA) are a family of methods which solve optimization problems by imitating the main characteristics of natural evolution: the survival of the better adapted member. Taking into account this idea, populations of designs are generated through the operators of selection, crossover and mutation, which are inspired in the fundamentals of genetics. Each generation of designs is expected to be better (best fitted) than its parents. The first part of this work is to select the most suitable GA version to optimize a composite material stringer under compression load. A simple stringer, with a known optimum, is used

as a benchmark to carry out the comparison.

Once the most suitable GA has been chosen, an accurate and more complex model of a stiffened panel with a run-out stringer under tensile load is considered. A run-out is a type of stringer termination with a cut-out with a certain angle. This type of termination introduces perpendicular deflection to the panel which leads to a more complex design and analysis process. To analyse the effect of some geometrical parameters on the ultimate tensile loads, four different run-out geometries were modelled using Finite Element (FE). In this virtual test the interface of panel-stringer set is simulated with cohesive elements, so the crack onset and its progression can be analysed. After completing all the simulations, the conclusions help to define some geometric guidelines to improve the damage tolerance of the set panel-stringer while the failure mechanism is understood.

Finally, a method to optimize a damage tolerant design of a stringer run-out under tensile load is proposed. In this case, the FE model is simplified to reduce the computation time. Thus, cohesive elements in the interface of the set panel-stringer are not used but another crack progression technique is proposed: Virtual Crack Closure Technique (VCCT). Once the model is simplified, a set of different geometrical configurations is generated to produce a metamodel of the test. Metamodeling is a technique to replace partially the FE model solution. Thus, at each iteration of the optimization method, or in the case of the GAs, for each individual at each generation, instead of solving a complete FE model to obtain the objective function, a much simpler mathematical function (the metamodel) is used so computational time is reduced considerably. In our case, the chosen metamodel is a Radial Basis Function (RBF). Next, the optimization of the design is performed using the created RBF and some new guidelines about run-out configurations are derived.

Resum

L'ús de panells rigiditzats a la indústria aeronàutica i aeroespacial ha anat creixent les darreres dècades. Aquests panells obtenen un augment de la rigidesa sense un increment substancial del seu pes gràcies als rigiditzadors que s'hi afegeixen. La varietat de rigiditzadors i el seu ús estès ha fet que sigui un camp d'estudi amb una presència notable a la literatura científica. Per altra banda, el creixement exponencial de l'ús dels materials compòsits en els últims anys també ha tingut una forta incidència en aquests components estructurals i en la indústria en general. Aquest tipus de materials estan formats a partir de dos materials constituents (anomenats matriu i reforç) que units ofereixen unes propietats completament diferents i millorades als dos materials per separat. En conseqüència, l'obtenció d'un nou material fa aparèixer comportaments desconeguts fins al moment, com per exemple l'aparició de nous mecanismes de fallada. Aquests fets provoquen que el càlcul, anàlisi i assaig d'estructures de material compòsit sigui complex. Per aquest motiu, sumat a l'augment de potència de càlcul dels ordinadors, l'assaig virtual amb el mètode dels elements finits ha anat agafant una importància cabdal en el càlcul de components d'alta responsabilitat estructural. De la mateixa manera, l'intent de millorar els panells rigiditzats ha portat a utilitzar mètodes d'optimització. Modificant diferents paràmetres, siguin geomètrics, de càrrega o de definició de materials, es busca dissenyar panells rigiditzats per realitzar una tasca desitjada de manera òptima.

Els Algoritmes Genètics (AG) són una família de mètodes que solucionen problemes d'optimització basant-se en la selecció natural, és a dir, només sobreviuen els més ben adaptats. Prenent de model aquesta idea, es generen poblacions de dissenys mitjançant els operadors de selecció, encreuament i mutació, els quals estan inspirats en conceptes genètics. S'espera que cada generació de dissenys sigui millor (més ben adaptada) que els seus predecessors. La primera part d'aquest treball es concentra en seleccionar la variant d'AG més favorable per a l'optimització d'un rigiditzador de material compòsit sotmès a càrregues de compressió. Un rigiditzador senzill, amb l'òptim conegut, és pres com a punt de referència per realitzar la comparació.

Un cop escollit l'AG més favorable, es procedeix a crear un model precís i més complex d'un panell rigiditzat amb un rigiditzador amb *run-out* sotmès a tracció. Un *run-out* és un tipus de terminació de la costella del rigiditzador amb un tall en angle. Aquesta classe de terminació genera un tipus de deflexió perpendicular al panell que dificulta el seu disseny i complica l'estudi de l'estructura. Per analitzar l'efecte que alguns paràmetres geomètrics tenen sobre la força de tensió última, es creen quatre models d'Elements Finits (EF). En aquest assaig virtual se simula la unió del conjunt panell-rigiditzador amb elements cohesius per poder captar l'inici i la progressió de l'esquerda. Després de completar totes les simulacions, les conclusions ajuden a donar algunes indicacions de disseny geomètric per millorar la tolerància al dany del conjunt panell-rigiditzador a part d'entendre i predir els seus mecanismes de fallada.

Finalment, es proposa un mètode per optimitzar un disseny tolerant al dany d'un rigiditzador *run-out* sotmès a tracció. En aquest cas el model d'EF és simplificat per poder reduir el temps de càlcul. De la mateixa manera, no s'apliquen elements cohesius a la unió del conjunt panell-rigiditzador sinó que es fa servir una altra tècnica de càlcul de la progressió d'esquerda, l'anomenat VCCT (de l'anglès *Virtual Crack Closure Technique*). Un cop simplificat el model es generen un conjunt de casos per tal de construir un metamodel de l'assaig. El metamodelatge (*metamodeling*) és una tècnica per substituir parcialment la solució d'un model d'EF complet. Així, a cada iteració de l'optimització o, en el cas dels AGs, per cada individu a cada generació, s'utilitza el metamodel en comptes del model d'EF. D'aquesta manera, el temps de càlcul es redueix considerablement. En el nostre cas el metamodel triat és una funció de base radial (*radial basis function*). Tot seguit, s'optimitza el disseny emprant la funció de base radial creada i amb els resultats s'obtenen noves línies de disseny per al *run-out*.

Resumen

El uso de paneles rigidizados en la industria aeronáutica y espacial ha crecido en las ultimas décadas. Estos paneles obtiene un aumento de la rigidez, sin un incremento substancial de su peso, gracias a los rigidizadores que son añadidos a este. La variedad de rigidizadores y su uso extendido ha hecho que sea un campo de estudio con una presencia notable en la literatura científica. Por otro lado, el crecimiento exponencial del uso de los materiales compuestos en los últimos años también ha tenido una fuerte incidencia en estos componentes estructurales y en la industria en general. Este tipo de materiales están formados a partir de dos materiales constituyentes (llamados matriz y refuerzo) que, unidos, ofrecen unas propiedades completamente diferentes y mejoradas a los dos materiales por separado. En consecuencia, la obtención de un nuevo material hace aparecer comportamientos desconocidos hasta el momento, como por ejemplo la aparición de nuevos mecanismos de fallo. Estos hechos provocan que el cálculo, análisis y ensayo de estructuras de material compuesto sean complejos. Por este motivo, sumado al aumento de potencia de cálculo de los ordenadores, el ensayo virtual con el método de los elementos finitos ha ido cogiendo una importancia capital en el cálculo de componentes de alta responsabilidad estructural. Del mismo modo, el intento de mejorar los paneles rigidizados ha llevado a utilizar métodos de optimización. Modificando diferentes parámetros, sean geométricos, de carga o de definición de materiales, se busca diseñar paneles rigidizados para realizar una tarea designada de forma óptima.

Los Algoritmos Genéticos (AG) son una familia de métodos que solucionan problemas de optimización basándose en la selección natural, es decir, sólo sobreviven los mejor adaptados. Tomando de modelo esta idea, se generan poblaciones de diseños mediante los operadores de selección, cruce y mutación, los cuales están inspirados en conceptos genéticos. Se espera que cada generación de diseños sea mejor (más adaptada) que sus precedentes. La primera parte de este trabajo se basa en seleccionar la variante de Algoritmo Genético (AG) más favorable para la optimización de un rigidizador de material compuesto sometido a cargas de compresión. Un rigidizador sencillo, con el óptimo conocido, es tomado

como punto de referencia para realizar la comparación.

Una vez escogido el AG más favorable, se procede a crear un modelo preciso y más complejo de un panel rigidizado con un rigidizador en *run-out* sometido a tracción. Un *run-out* es un tipo de terminación en la costilla del rigidizador con un corte en ángulo. Esta clase de terminación genera un tipo de deflexión perpendicular al panel que dificulta su diseño y complica el estudio de la estructura. Para analizar el efecto que algunos parámetros geométricos tienen sobre la fuerza de tensión última, se crean cuatro modelos de Elementos Finitos (EF). En este ensayo virtual se simula la unión del conjunto panel-rigidizador con elementos cohesivos para poder captar el inicio y progresión de la grieta. Después de completar todas las simulaciones, las conclusiones ayudan a dar algunas indicaciones de diseño geométrico para mejorar la tolerancia al daño del conjunto panel-rigidizador, aparte de entender y predecir sus mecanismos de fallo.

Finalmente, se propone un método para optimizar un diseño tolerante al daño de un rigidizador *run-out* sometido a tracción. En este caso el modelo de EF se simplifica para poder reducir el tiempo computacional. Del mismo modo, no se aplican elementos cohesivos en la unión del conjunto panel-rigidizador sino que se usa otra técnica de cálculo de progresión de grieta, llamado VCCT (del inglés *Virtual Crack Closure Technique*). Una vez simplificado el modelo, se generan un conjunto de casos para construir un metamodelo del ensayo. El metamodelado (*metamodeling*) es una técnica para substituir parcialmente la solución de un modelo de EF completo. Así, en cada iteración de la optimización o, en el caso de los AGs, por cada individuo en cada generación, se utiliza el metamodelo en vez del modelo de EF. De esta manera, el tiempo de cálculo se reduce considerablemente. En nuestro caso el metamodelo escogido es una función de base radial (*radial basis function*). Seguidamente, se optimiza la función de base radial creada y con los resultados se obtienen nuevas líneas de diseño para el *run-out*.

Chapter 1

Introduction and objectives

1.1 Introduction

In the present chapter, an overview of the topics covered in this thesis is presented. Finally, a summary of the objectives of this work is exposed.

This thesis is devised as a compendium of manuscripts published in (or submitted to) indexed scientific journals. Chapter 2 is the transcription of the published paper "A comparative study of genetic algorithms for the multi-objective optimization of composite stringers under compression loads". Then, Chapter 3 is the submitted manuscript "Virtual test of different types of composite stringer run-outs under tensile load". Next, the submitted paper "Damage tolerance optimization of composite stringer run-out under tensile load" is exposed in Chapter 4.

Finally, the Chapter 5 presents the main conclusions of this thesis and the future works.

1.2 Stiffened panels

During the last decade, the industrial application of the composite materials has been increasing. The aircraft/aeronautical industry is one of the most advanced industries with the use of these materials. A common structural solution used in fuselages and wings of aircrafts are panels stiffened with stringers. These panels, named stiffened panels (Fig. 1.1), provide a high increment of the stiffness with a small addition of weight. The stringers are added in the panel with adhesive, which can be designed with different shapes depending of the objective or geometry of the structure. Normally, this adhesive bonding is a critical point of the set panel-stringer. Thus, it needs a detailed analysis to know the behaviour of the set: onset damage, crack propagation, etc.

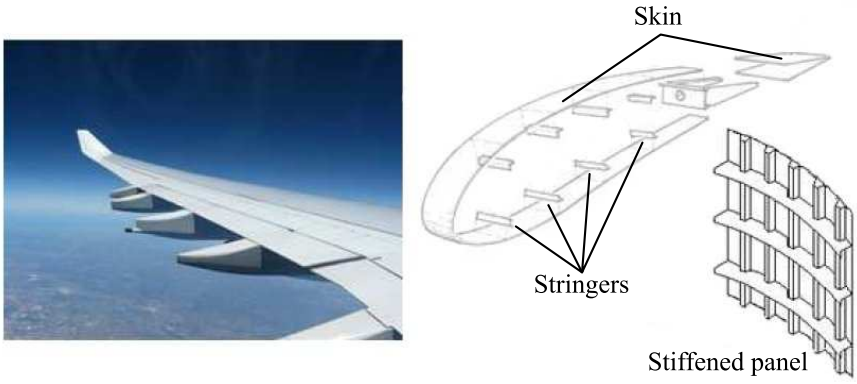

Figure 1.1: Stiffened panels.

In addition, some geometric requirements of the design, may lead to the introduction of a run-out in the stringer. A run-out is a cut-out with a certain angle at the end of the rib (Fig. 1.2), which generates an important increment of the difficulty in the study of the interface panel-stringer.

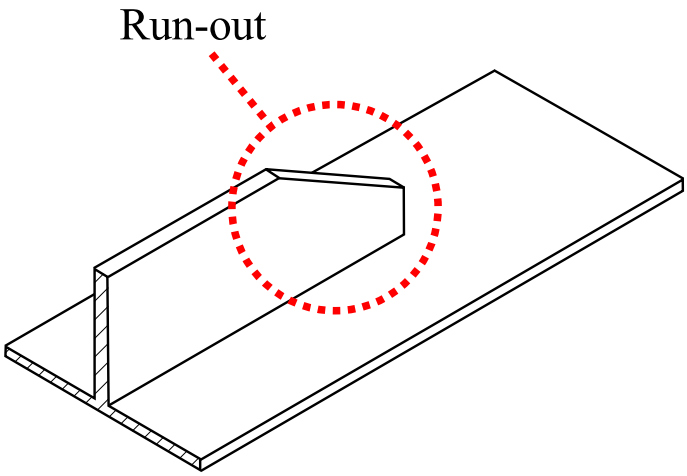

Figure 1.2: Example of stringer run-out.

1.3 Virtual tests

In the last years, the raise of the computer power has increased use of powerful computational techniques. The application of the so-called virtual tests is a frequently used method to reduce the cost and the development time in the design of composite structures (Fig. 1.3). On the other hand, the virtual testing is a tool to obtain a detailed and precise results of the behaviour of the complex structures and materials.

The virtual testing using Finite Element Method (FEM) is one of the main tools used in this work. In Chapters 2, 3 and 4 virtual tests are used to evaluate the behaviour of the real structures. Accurate models to analyse the adhesive bond of different stringer run-outs with a panel are presented in Chapter 3.

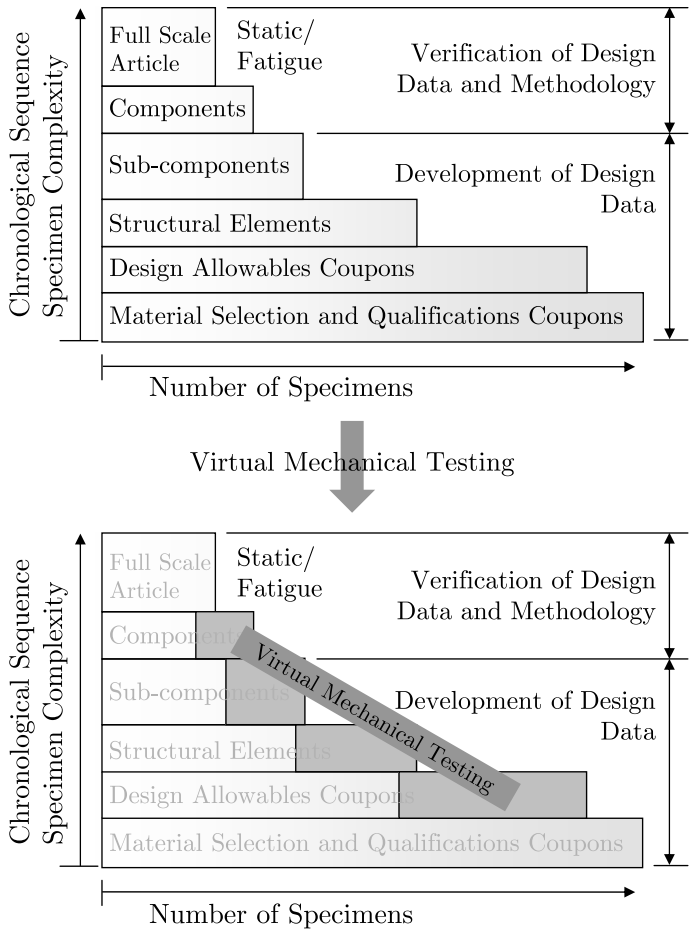

Figure 1.3: Building block integration of the certification methodology [1] and reduction on the test requirements through Virtual Testing.

1.4 Genetic algorithms

Another method to reduce the component development time and to improve of the structural response is design optimization. Some of the most used optimization methods are Genetic Algorithms (GA). The original formulation of GAs is based on the concept of natural evolution: the survival of the fittest member, i.e., the better adapted members have more possibilities to transmit their characteristics to future generations. The translation of this strategy into an algorithm is performed by means of three operators:

- *Selection operator* which randomly selects individuals with high fitness to whom the next operators will be applied. This set is named mating pool.
- *Crossover operator* which performs the exchange of some characteristics between two or more members of the mating pool (Fig. 1.4(a)). Two individuals, called parents,

exchange some characteristics to generate two new members, called children.

- *Mutation operator* is implemented to save the process of losing genetic information which would be relevant for the optimal solution during crossover (Fig. 1.4(b)). Random changes are applied in some individuals during this process to preserve diversity in the population.

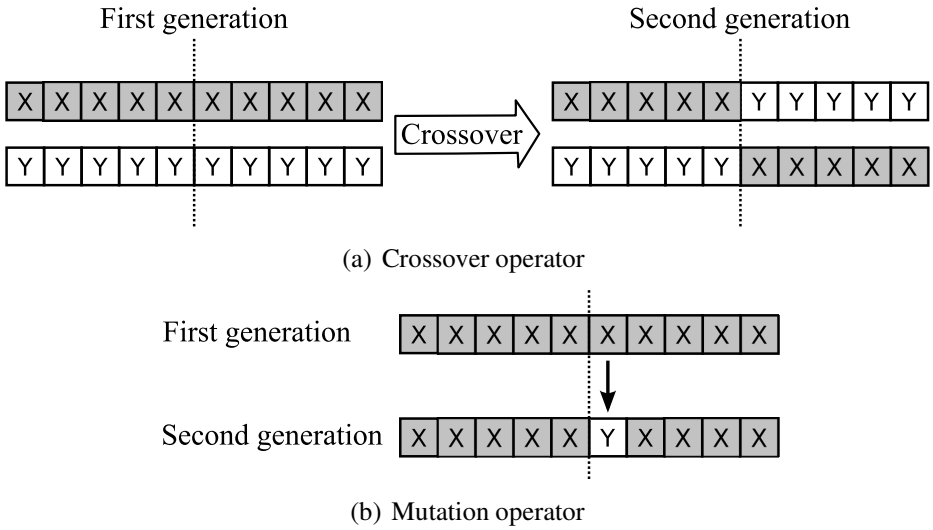

Figure 1.4: Two operators of GAs.

Nowadays, there are different types of GAs. For this reason, in Chapter 2 a comparison between three GAs is carried out to select the most recommended GA in a specific case of study. One of these is selected to achieve future optimizations (Chapter 4).

1.5 Metamodeling

In some analysis, for example the use of the optimization methods, a large number of virtual tests are needed. A considerable number of full analysis with finite elements requires a huge computational time. Accordingly, in these cases the creation of a metamodel is used to reduce the computational time without an appreciable loss of precision. Metamodeling (or surrogate modeling) offers approximations from high-fidelity models.

In Chapter 4 a metamodel is created to replace the FEM of stringer run-out with a noticeable computation cost. Radial Basis Functions (RBFs) are computed and compared to chose the most accurate. Then, the results of the selected RBF are verified to ensure their veracity. Finally, two different optimization methods are used to provide some guidelines to design a stringer run-out.

1.6 Objectives

The global objective of this work is to investigate the influence of the stringers in stiffened panels and to use optimization techniques to improve their damage tolerance.

For this reason, the specific objectives of this study are:

- To use and to compare different GAs to choose the best one to apply in structures which use composite stringers.
- To model stringer-panel sets with different geometries of run-outs, using cohesive elements in the longitudinal midplane of stringer-panel set to perform the evolution of the damage.
- To analyse a stringer run-out to understand the influence of their geometric variables in the failure of the stringer-panel set.
- To generate a metamodel to reduce the computational time of the model.
- To apply different optimization techniques to improve the damage tolerance of stringer run-outs.

Chapter 2

A comparative study of genetic algorithms for the multi-objective optimization of composite stringers under compression loads

This chapter contains the transcription of the published paper:

P. Badalló, D. Trias, L. Marín, J. A. Mayugo. *A comparative study of genetic algorithms for the multi-objective optimization of composite stringers under compression loads*. Composites Part B: Engineering 2013; 47(0):130-136.

ISSN: 1359-8368

doi: 10.1016/j.compositesb.2012.10.037

Impact index 2.602; Journal 7 of 87; 1st quartile; Category: Engineering, Multidisciplinary.

The paper in journal format is shown in Appendix A

Abstract

Optimization methods are close to become a common task in the design process of many mechanical engineering fields, specially those related with the use of composite materials which offer the flexibility in the design of both the shape and the material properties and so, are very suitable to any optimization process. While nowadays there exist a large number of solution methods for optimization problems there is not much information about which method may be most reliable for a specific problem. Genetic Algorithms have been presented as a family of methods which can handle most of engineering problems. However, starting from a common basic set of rules many algorithms which differ slightly from each other have been implemented even in commercial software packages. This work presents a comparative study of three common Genetic Algorithms: Archive-based Micro Genetic Algorithm (AMGA), Neighborhood Cultivation Genetic Algorithm (NCGA) and Non-dominate Sorting Genetic Algorithm II (NSGA-II) considering three different strategies for the initial population. Their performance in terms of solution, computational time and number of generations was compared. The benchmark problem was the optimization of a T-shaped stringer commonly used in CFRP stiffened panels. The objectives of the optimization were to minimize the mass and to maximize the critical buckling load. The comparative study reveals that NSGA-II and AMGA seem the most suitable algorithms for this kind of problem.

2.1 Introduction

The use of optimization methods in the design of structural components has been growing in the last years and becoming a usual step in the mechanical engineering workflow of many companies, specially those focused on aircraft/aerospace composite structures whose characteristics frequently meet the paradigm of a standard multiobjective optimization problem. For this reason, a large amount of optimization strategies ([2–6] among others) are available in the literature nowadays.

A structure of special interest which has been the object of optimization routines are composite panels stiffened with stringers. The optimization of the set panel-stringer is of high interest since this kind of structure is widely used in the aircraft industry. For them, Genetic Algorithms (GAs) [7], a family of evolutionary algorithms, have been succesfully used, as reported in a large number of publications [8–12] among others. A case of special interest reported in the scientific literature is the optimization of the stacking sequence of composite laminates, for which GA have been used successfully [13, 14]. However, in situations where the stacking sequence cannot be considered as a design variable but a imposed requirement, the minimization of the weight is achieved with geometrical parameters [15, 16]. In that case, what makes different the optimization of composite structures from other materials is the use of failure mode based failure criteria such as Puck's [17] and LaRC [18]. These are in fact a set of failure criteria which assign a different index for the different failure modes under consideration. When they are included in optimization routines as non-smooth discontinuous constraints, the resulting optimization problem is very specific of composite materials, as can be concluded from some works analysing the effect of different failure criteria in the optimal solution [19–21].

The original formulation of GAs is based on the concept of natural evolution: the survival of the fittest member, i.e., the better adapted members have more possibilities to transmit their characteristics to future generations. The translation of this strategy into an algorithm is performed by means of three operators:

- *Selection operator* which selects individuals with high fitness to form the mating pool.
- *Crossover operator* which permits the exchange of some characteristics between two or more members of the mating pool. Two individuals, called parents, exchange some characteristics to generate two new members, called children.
- *Mutation operator* is implemented to save the process of losing genetic information during crossover. Random changes are applied in some individuals during the mutation

process to preserve diversity in the population.

Although these three operators are the basis of a GA, there exist a large number of variations which implement different encodings, different selection operators, different methods for mating pairs or different strategies for mutation [22]. The behaviour of a specific GA depends on the studied problem [23, 24] and the design variables [25], for this reason, some previous experience or some comparative analysis is needed for selecting one GA out of a set of implemented GAs. Some comparative studies of evolutionary algorithms with different industrial cases have been already carried out, [26, 27] for example. These studies reveal that the best GA is different for each kind of problem.

A good choice when using GAs for the optimization of composite stiffened panels is a GA specifically designed for them, for example [28] and [29]. However, most of engineers are not familiar with the implementation of such algorithms and a commercial software with the most common GAs already implemented is a recommended option to carry out the optimization. In that case, a comparison of the most used GAs is a necessity for the choice as well.

The solution of the multi-objective optimization problem is linked to the concepts of dominance and non-dominance. When an individual is non-dominated it is a member of the Pareto's front, which is the set of possible optimal solutions. A candidate to solution **A** dominates candidate **B** if the conditions of Eq. 2.1 are fulfilled. On the other hand, if the Eq. 2.2 is satisfied **A** and **C** are considered non-dominated candidates.

$$f_i(\mathbf{A}) \prec f_i(\mathbf{B}) \leftrightarrow \Big(f_1(\mathbf{A}) < f_1(\mathbf{B})\Big) \wedge \Big(f_2(\mathbf{A}) < f_2(\mathbf{B})\Big) \tag{2.1}$$

$$f_i(\mathbf{A}) \sim f_i(\mathbf{C}) \leftrightarrow \Big((f_i(\mathbf{A}) \nleq f_i(\mathbf{C})\Big) \wedge \Big(f_i(\mathbf{A}) \ngeq f_i(\mathbf{C})\Big) \tag{2.2}$$

In this paper a comparative study of composite stringers under compression loads with three different GAs is carried out. The chosen three, implemented in software Isight™ [30], are: Archive-based Micro Genetic Algorithm (AMGA) [31], Neighborhood Cultivation Genetic Algorithm (NCGA) [32] and Non-dominate Sorting Genetic Algorithm II (NSGA-II) [33]. The main differences between these GAs are listed below:

- *NSGA-II*: After the creation of the parent population, sorting based on the non-dominance is used. A fitness (equal to non-domination level) is fixed in each solution. The best individuals of this ranking are used to create the new population using the selection, crossover and mutation operators.

- *AMGA*: This algorithm uses a small population size and creates an external archive with the best solutions obtained, which is updated every iteration. AMGA employs the concept of the non-dominance ranking of NSGA-II and it creates the parent population from the archive with the method of SPEA2 [34]. The mating pool is a derivation of the binary tournament selection method of NSGA-II. The use of the archive permits to obtain a large number of non-dominated points at the end of the simulation. AMGA is a GA highly based in NSGA-II.

- *NCGA*: A neighborhood crossover mechanism is added in the normal mechanisms of GAs which it improves the crossover operator. The pair of individuals to perform crossover is not randomly chosen, but the individuals who are close each other in the objective space are selected.

A T-shape stringer is used as a benchmark because of its simple geometry with only two design variables (subsection 2.2.1) and because of its real-life interest in the design of stiffened panels. A preliminary study of the stringer is performed (subsection 2.2.3) which permits to know the approximated optimal result. These structures are used for their compression behaviour with low weight. For this reason, the objectives are both the maximization of the critical buckling load (P_{cr}) and the minimization of the stringer mass (m). In these cases, P_{cr} normally is most important for these structures and their design is in function of it. Then, in the optimization process is prioritized the P_{cr} than the mass (details in section 2.3). Therefore, the previous optimal result is compared with the optimization results (section 2.4) to know the reliability of the GA. Finally, a GA is proposed to use in the solution of similar multi-objective optimization problems.

2.2 Benchmark problem

2.2.1 Specimen

In this study a composite material T-shape stringer has been analysed under compression load (Fig. 2.1). This geometry was selected since it provides both simplicity to run a benchmark and real life engineering interest.

The stringer is made from AS4/8552 pre-preg whose properties are described in Table 2.1. Stacking sequence is $[0/90/0_2/\pm 45]$ for the stringer base and $[\pm 45/0_2/90/0]_S$ for the stringer rib.

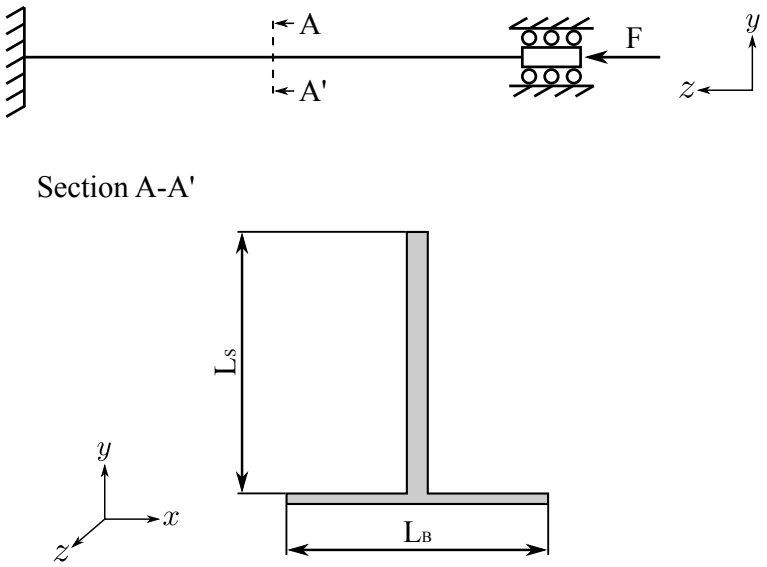

Figure 2.1: Stringer section and schematic representation of the test.

2.2.2 Virtual test

To carry out the optimization, a virtual test was modelled, using ABAQUS™ (Fig. 2.2). A compression load is applied on an end of the stringer and clamped by the other end. This compression load is applied by means of pottings, metallic elements where the stringer can be introduced and fixed with resin (Fig. 2.2). A potting only permits the displacement of the stringer base in X-axis and Y-axis in stringer rib. In the middle of the specimen a damaged zone was introduced to simulate the effects of an impact. This damaged zone is located in the stringer rib, in the middle of the specimen and it is modelled by reducing in a 50% the values of E_{xx} and X_{C}. The location of the damaged zone and the amount of properties reduction were obtained in a previous study [38]. It is added to simplify the finite element analysis (FEA) and to set the region where the first ply failure will appear. LaRC failure criteria is applied only in damaged zone to reduce computation time because it is known that the first ply failure will appear in the previously damaged zone. The elements used in mesh are S4 shell type (4-node shell element with full integration).

2.2.3 Preliminary study

A preliminary study aiming to determine the influence of design variables in the principal objective, P_{cr} and to obtain an approximated optimal solution was carried out. This results will be used to compare the performance of the analysed algorithms.

Individuals with different dimensions of the stringer base length (L_{B}) and the stringer rib

Property	Value	Units	Description
E_{xx}	135	GPa	Young's modulus in fiber direction.
E_{yy}	9.6	GPa	Young's modulus in transversal fiber direction.
E_{zz}	9.6	GPa	Estimated $E_{yy} = E_{zz}$. (transversally isotropic material).
ν_{xy}	0.32	-	Poisson's modulus in XY plane.
ν_{xz}	0.32	-	Estimated $\nu_{xy} = \nu_{xz}$. (transversally isotropic material).
ν_{yz}	0.487	-	Poisson's modulus in YZ plane.
G_{xy}	5.3	GPa	Shear modulus in XY plane.
G_{xz}	5.3	GPa	Estimated $G_{xy} = G_{xz}$ (transversally isotropic material).
G_{yz}	3.228	GPa	Shear modulus in YZ plane.
X_T	2207	MPa	Longitudinal tensile strength.
X_C	1531	MPa	Longitudinal compressive strength.
Y_T	80.7	MPa	Transverse tensile strength.
Y_C	199.8	MPa	Transverse compressive strength.
$S_{L_{UD}}$	114.5	MPa	In-plane shear strength.
$\mathcal{G}_{I_C}{}^{\star}$	0.2839	N/mm	Critical fracture energy in mode I.
$\mathcal{G}_{II_C}{}^{\dagger}$	1.0985	N/mm	Critical fracture energy in mode II.
ρ	$1.59 \cdot 10^{-9}$	T/mm^3	Density.

* Source: [36]
† Source: [37]

Table 2.1: AS4/8552 properties. Source: [35], unless otherwise stated.

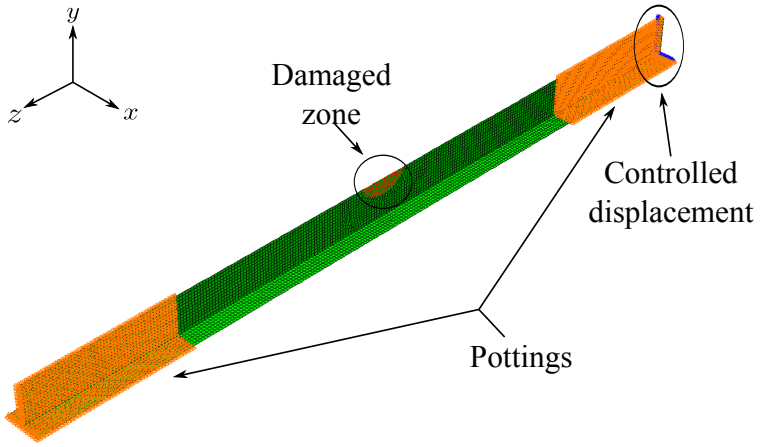

Figure 2.2: Benchmark problem.

length (L_S) were distributed in design space and FEA was run for each individual. A design was considered unfeasible if the specimen damage started.

P_{cr} was calculated with the expression:

$$P_{cr} = RF \cdot \lambda \tag{2.3}$$

where RF is reaction force supported by the stringer and λ is the first stringer eigenvalue. Once all distributed cases were executed the influence of each design variable was analysed. As shown in Fig. 2.3 P_{cr} grows directly proportional to L_B until $L_B \simeq 29$ mm, when it starts to decrease. On the other hand, P_{cr} decreases inversely proportional to L_S (Fig. 2.4). This is because P_{cr} is dependent of λ, which is related to the vibration mode. At the same time, the vibration modes are dependent on the inertia. In our system of reference, the lowest inertia is I_{yy} and, for this reason, the specimen rotates respect to Y-axis. An increment of L_B generates an increment of I_{yy}, so the P_{cr} grows as well. When $L_B \simeq 29$ mm the vibration mode changes and λ decreases, and so does the P_{cr}.

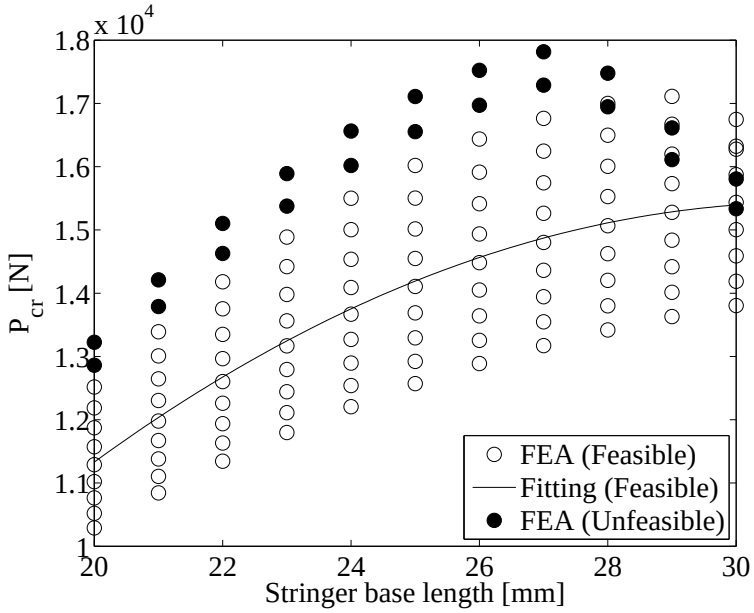

Figure 2.3: P_{cr} vs. L_B.

When P_{cr} is plotted against L_B and L_S (Fig. 2.5) a peak is observed. This peak indicates the highest P_{cr}, that is the approximated optimal solution. This previous optimal solution has the values L_B approximately between 28 and 29 mm and L_S between 21 and 22 mm.

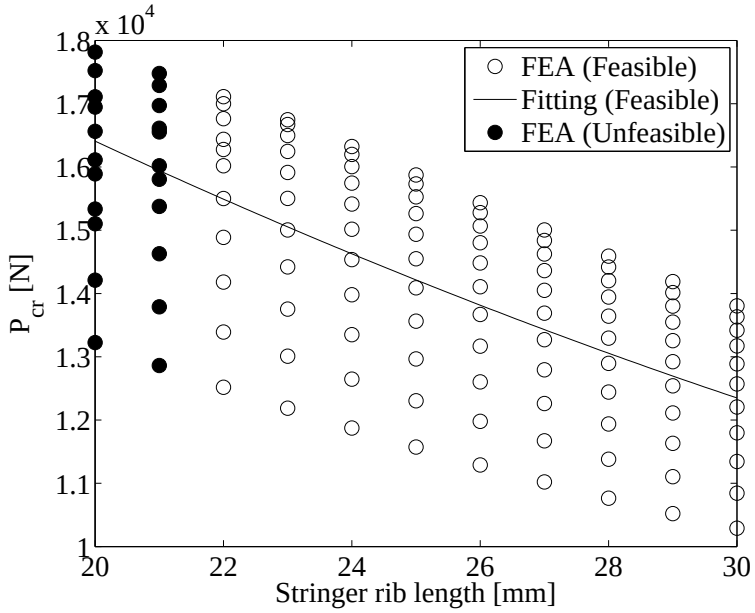

Figure 2.4: P_{cr} vs. L_{S}.

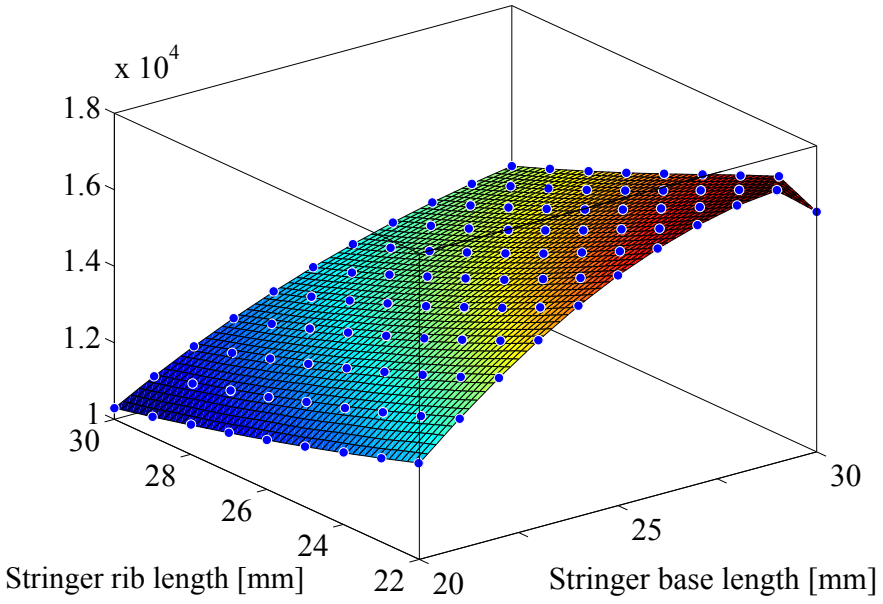

Figure 2.5: P_{cr} vs. L_{B} and L_{S}.

2.3 Multi-objective optimization

The two objectives of the optimization problem are to maximize P_{cr} and to minimize m, that is $f_1(\mathbf{x}) = -P_{\text{cr}}$ and $f_2(\mathbf{x}) = m$. The design variables are the length of the base (L_{B}) and the rib (L_{S}) of the stringer.

The optimization problem is defined as:

$$\begin{aligned} &\text{Minimize} && F_{\text{obj}}\left(f_1(\mathbf{x}), f_2(\mathbf{x})\right) \\ &\text{Subject to} && g(\mathbf{x}) > 0 \\ & && 20 \leq \mathrm{x}_i \leq 30 \qquad i = 1, 2 \end{aligned} \tag{2.4}$$

where $\mathbf{x} = (L_{\text{B}}, L_{\text{S}})$, $g(\mathbf{x}) = 1 - FI(\mathbf{x})$ and $FI(\mathbf{x})$ is the LaRC failure index.

Subsequently, the objective function (F_{obj}) is described:

$$F_{\text{obj}} = \sum \left(\frac{f_i(\mathbf{x}) \cdot w_i}{s_i} \right) \tag{2.5}$$

where $f_i(\mathbf{x})$ are the different objectives, w_i and s_i the weight and scale factors for each objective, respectively. To give priority to P_{cr} the values of the weights w_1 and w_2 are set 0.7

and 0.3, respectively.

The commercial software Isight™, with several optimization methods implemented, was used to solve the multi-objective optimization problem of Eq. 2.4. This software implements Eq. 2.5 which is used as a post-processing to extract the optimal solution from the Pareto front delivered by the GAs. Isight™ permits to link ABAQUS™ with the chosen optimization method and to calculate the P_{cr} for each individual. ABAQUS™ analyses the different geometries (individuals) computed for the optimization method. RF, λ, m and FI of the individuals are calculated by ABAQUS™ and P_{cr} by Isight™. Each GA has the same scheme. The used computer is a HP Compaq dx2400 Microtower with an Intel® Core™ 2 Quad CPU Q8200 with 2.33GHz, 4GB of RAM, MS Windows XP Professional x64 Edition, Isight™ 5.5 and ABAQUS™ 6.9-3.
Once the optimization scheme was designed the different GAs were executed with different initiation modes. These modes set how the initial population is generated:

- *Distributed population* (DP): Equally spaced points in the design space are created.
- *Random* (R): A cloud of random cases is generated.
- *Initial solution* (IS): The starting initial population is a random cloud near to an initial geometry. For the analysed case it was set $L_{\text{B}} = 24$ mm and $L_{\text{S}} = 25$ mm.

The GA parameters are fixed to analyse each GA with the same conditions. The values of parameters are listed below:

- *Number of generations*: 25
- *Generation size*: 16 individuals
- *Selection rate*: 50%
- *Crossover probability*: 90%
- *Mutation probability*: 50%

These parameters generate 400 individuals for each GA and each initiation mode. AMGA is an exception, since it needs a different initial generation. For this reason, the value of initial population of AMGA is 40. This modification forces to change the number of generations to 24 to obtain the same approximated number of cases. On the other hand, Isight™ does not

permit the IS mode with NCGA. Because of the fact that the GAs have a random component, related to crossover and mutation operators, each GA and each initiation mode was executed five times.

The executions for each GA and initiation mode are performed in random order to reduce the effect that other processes running in the computer might have on the results of the computational experiment.

2.4 Results and Discussion

The comparison of the different algorithms is performed in terms of: obtained solution, computational time and number of generations to obtain the optimal. When an optimal individual does not improve after a specific generation, it is considered that this generation has reached the optimum. The obtained results are listed in Table 2.2.

All values L_{B} and L_{S} of the Table 2.2 are in agreement with the previous study, except four individuals. These four individuals, all in NCGA and DP mode (iterations 1, 2, 3 and 4), obtain a lower value of F_{obj} than the individuals of other GAs and initiation modes. A priori, this fact indicates that NCGA is the GA with the worst results, particularly with DP mode.

The mean, median and standard deviation were calculated for each GA and each variable (Table 2.3). This table shows that there are non-significant differences between the GAs for time variable, since the differences of mean are lower than 1%. Then, the mean of F_{obj} in NCGA is 2.44% and 2.26% lower than AMGA and NSGA-II respectively. Again, NCGA delivers different and lower results of the F_{obj}. However, AMGA and NSGA-II have a similar result with 0.18% of difference. NSGA-II achieves the best result of number of generations which is 9.91% lower than to AMGA, which occupies the second place. On the other hand, NCGA obtains a number of generations 2.83% lower than AMGA and 7.28% greater than NSGA-II.

To determine what statistical test is the most accurate to handle all data, the data type needs to be identified. The Kolmogorov-Smirnov test is used to determine the normality of the data (each GA and each initiation mode independently). This test concluded that all the sets of data are non-normal populations. In this situation, a non-parametric test is recommended. Furthermore, as reported in [39], non-parametric tests are specially useful for the analysis of evolutionary algorithms, in this case GAs. The Mann-Whitney U-test (also known as Wilcoxon rank sum test) was used to compare the data. The null hypothesis of the Mann-Whitney test is that compared populations have identical distributions with equal median, against the alternative of different medians. This test has to be applied by facing the data

GA	Initiation	Iteration	P_{cr} [kN]	m [g]	L_B [mm]	L_S [mm]	F_{obj}	Time [min]	Generations
AMGA	DP	1	17.386	65.24	28.49	21.37	67.36	580.8	14
		2	17.356	65.41	28.53	21.44	67.16	585.6	23
		3	17.340	65.54	28.58	21.49	67.04	597.5	23
		4	17.359	65.16	28.36	21.39	67.25	586.8	23
		5	17.335	65.25	28.36	21.45	67.09	590.7	22
	R	1	17.350	65.41	28.51	21.45	67.13	586.4	23
		2	17.394	65.19	28.47	21.35	67.41	575.6	23
		3	17.365	65.02	28.28	21.36	67.32	583.6	20
		4	17.385	65.26	28.51	21.38	67.35	584.2	20
		5	17.355	65.73	28.78	21.49	67.06	581.1	23
	IS	1	17.342	65.55	28.59	21.45	67.04	574.1	24
		2	17.362	65.31	28.48	21.42	67.22	582.9	22
		3	17.353	65.35	28.48	21.43	67.16	576.5	21
		4	17.386	65.28	28.52	21.38	67.35	584.0	19
		5	17.344	64.91	28.15	21.36	67.24	581.6	18
NCGA	DP	1	17.198	66.70	29.04	21.89	65.98	586.0	24
		2	16.948	68.08	29.34	22.50	64.31	596.3	22
		3	16.617	68.94	29.02	23.13	62.40	581.4	20
		4	16.877	67.55	28.75	22.50	64.12	577.9	20
		5	17.156	66.24	28.58	21.86	65.91	581.1	22
	R	1	17.103	65.01	27.66	21.66	66.02	568.7	16
		2	17.303	65.35	28.34	21.50	66.91	579.2	22
		3	17.313	65.38	28.39	21.49	66.95	581.8	22
		4	17.112	64.62	27.45	21.55	66.17	580.9	20
		5	17.303	65.14	28.20	21.46	66.97	577.2	18
NSGA-II	DP	1	17.364	65.23	28.42	21.40	67.25	578.1	23
		2	17.361	65.33	28.58	21.42	67.21	575.6	19
		3	17.322	65.09	28.22	21.42	67.08	587.9	21
		4	17.357	65.38	28.51	21.44	67.17	581.8	21
		5	17.319	64.98	28.13	21.41	67.09	588.9	20
	R	1	17.363	65.50	28.62	21.45	67.16	581.1	21
		2	17.375	65.05	28.32	21.35	67.36	577.7	16
		3	17.301	64.99	28.10	21.43	67.00	579.4	14
		4	17.372	65.41	28.58	21.42	67.24	580.7	17
		5	17.370	65.51	28.65	21.44	67.19	592.1	10
	IS	1	17.377	65.15	28.40	21.37	67.34	570.7	19
		2	17.394	65.44	28.58	21.44	67.19	580.1	21
		3	17.213	64.45	27.56	21.40	66.73	578.2	20
		4	17.151	64.19	27.29	21.40	66.49	563.7	22
		5	17.265	64.71	27.84	21.41	66.91	577.3	22

Table 2.2: Summary of obtained results.

two by two which leads to face each GA to the others. This process was repeated in each comparison variable. The results of the Mann-Whitney test are in Table 2.4, where $=$ is null hypothesis acceptance and $\neq$ is null hypothesis rejection.

Results of the test reflect that the time values are equal for all GA. Furthermore, an equal distribution is observed for F_{obj} in AMGA and NSGA-II, while different results are detected

Variable	GA	Mean	Median	Stand. dev.
F_{obj}	AMGA	67.21	67.22	0.13
	NCGA	65.57	66.00	1.50
	NSGA-II	67.09	67.17	0.23
Time	AMGA	583.4	583.6	5.9
	NCGA	581.0	581.0	6.9
	NSGA-II	579.6	579.4	6.9
Number of generations	AMGA	21.2	22	2.7
	NCGA	20.6	21	2.3
	NSGA-II	19.1	20	3.5

Table 2.3: Statistics of the results.

		AMGA	NCGA	NSGA-II
F_{obj}	AMGA		$\neq$	$=$
	NCGA	$\neq$		$\neq$
	NSGA-II	$=$	$\neq$	
Time	AMGA		$=$	$=$
	NCGA	$=$		$=$
	NSGA-II	$=$	$=$	
Number of generations	AMGA		$=$	$\neq$
	NCGA	$=$		$=$
	NSGA-II	$\neq$	$=$	

Table 2.4: Mann-Whitney test results.

in NCGA. The lowest value of F_{obj} in NCGA (shown in Table 2.3) indicates that AMGA and NSGA-II are a good option to obtain a high and similar value of F_{obj}. On the other hand, an unequal distribution is obtained for the value of number of generations in AMGA and NSGA-II. Moreover, NCGA is similar to AMGA and NSGA-II. The values of Table 2.3 reveal that the number of generations for NCGA are approximately equidistant between AMGA and NSGA-II. For this reason, NCGA is similar to AMGA and NSGA-II but these are different among them. NSGA-II needs less generations to obtain the optimal. However, a high standard deviation indicates that a random component exists. Additionally, the initiation mode was studied. The distribution of the studied cases in each GA and each initiation mode was analysed and the optimum evolution as well. The most representative cases are shown in Fig. 2.6.

Fig. 2.6(a) depicts the lines of distributed cases and the fact that the initial optimal solution is close to the final solution. This means that a DP mode enables the GA to achieve a faster

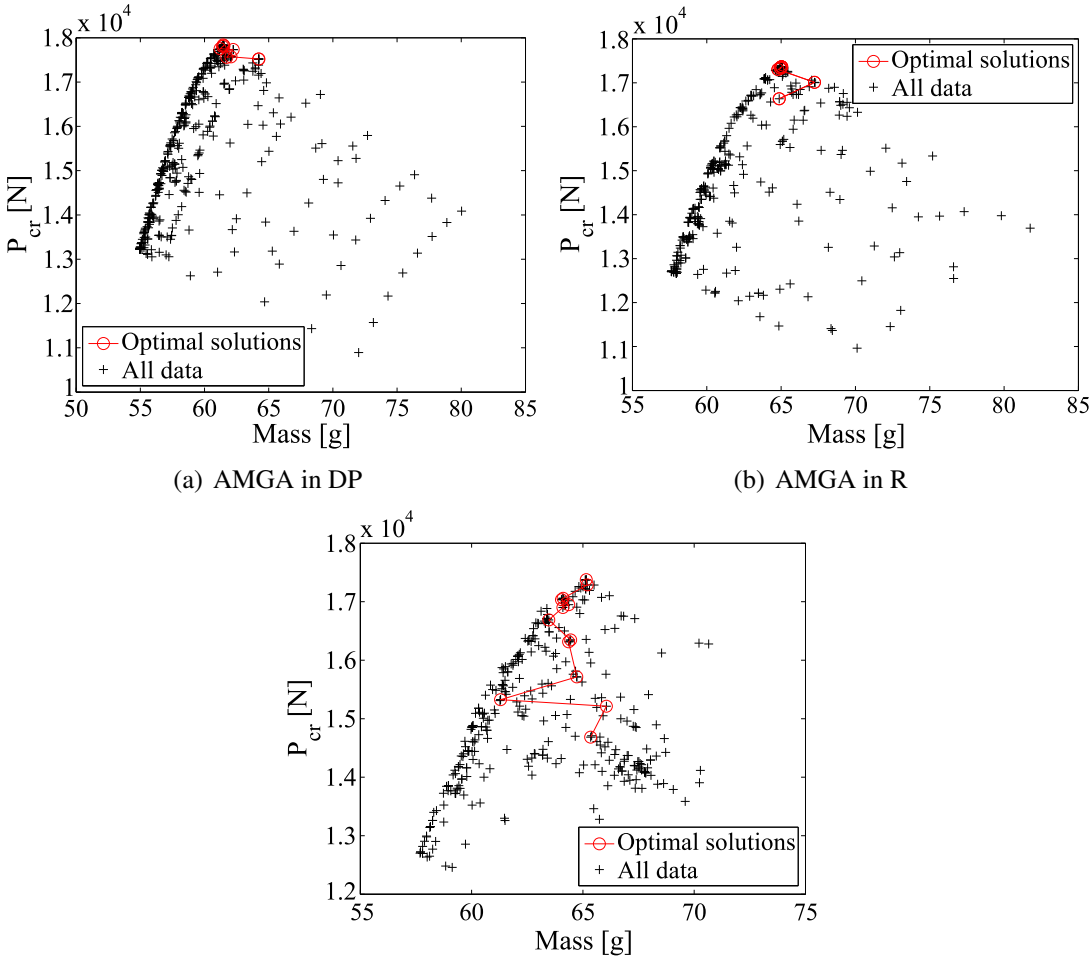

(a) AMGA in DP

(b) AMGA in R

(c) NSGA-II in IS

Figure 2.6: Evolution of the optimums.

optimal solution. On the other hand, a R mode has an expected random distribution (Fig. 2.6(b)). A possible remote initial optimal solution is the problem of a R mode, which may delay the arrival at the optimum. Finally, the first optimal solution is usually further from the final optimum in IS mode (Fig. 2.6(c)). This last initiation mode is recommended to improve a previous result.

2.5 Conclusion

A process to compare three GAs for the solution of multi-objective optimization problem of a simple composite material structure has been presented. A T-shape composite stringer under compression loads has been used as a benchmark for three different GA: AMGA, NCGA and NSGA-II. Moreover, a preliminary study of the specimen has been carried out to

demonstrate that all the GAs reach the optimal solution.
An analysis of the results aids to recognize the first differences between the GAs. Therefore, a lower value of F_{obj} is observed in NCGA. A non-parametric test (Mann-Whitney U-test) has been used to compare the equality or inequality of the results. This test evidences that the computing time is independent on the GA used for the calculation because all the time values are similar. This conclusion might be affected by the use of a reduced number of design variables. On the other hand, both the AMGA and the NSGA-II achieve a high and similar value of F_{obj}. The lowest number of generations is obtained by NCGA and NSGA-II. Finally, the different initiation mode (DP, R and IS) has been analysed to appreciate the differences among them.
In conclusion, the results of F_{obj} and the number of generations indicate that the most recommended GAs for similar structural cases are NSGA-II and AMGA, because they give similar results.

Acknowledgments

The authors wish to acknowledge the Ministerio de Ciencia e Innovación for the funding of the project DPI2009-08048 and particularly to Universitat de Girona for the research grant coded as BR2011/02.

Chapter 3

Virtual test of different types of composite stringer run-outs under tensile load

This chapter contains the transcription of the submitted paper:

P. Badalló, D. Trias, L. Marín, Ll. Ripoll. *Virtual test of different types of composite stringer run-outs under tensile load*. Engineering Failure Analysis.

Impact factor 1.130; Journal 8 of 33; 1st quartile; Category: Materials Science, Characterization & Testing.

Abstract

The use of run-outs, due to requirements of the design, is a common practice in the aircraft/aeronautical industry. Nowadays, there exists a large number of run-out geometries as a response to different structural objectives. The choice should be based on the global and local behaviour of the stringer-panel interface but this information is rarely reported. In this study, four types of run-out are considered, based on the variation of two design parameters. These run-out have been analysed and compared with experimental results published by other authors. The analysis takes into account: the damage on the interface, the evolution of the crack, the displacement of the panel, the failure modes and the induced stresses. A detailed virtual test with cohesive elements has been carried out to simulate the behaviour of the interface of these four run-out geometries to permit a better selection of the design depending on the necessities.

3.1 Introduction

The use of composite materials in aircraft/aerospace structures has been growing in the last years. However, the difficulty in predicting their service life implies a large number of tests in real-size structural components. The application of the so-called virtual test aims at reducing the cost and development time in the design of composite structures by replacing an amount of real tests by simulated ones. This approach has been used frequently in the recent years for typical aircraft subcomponents such as stringer stiffened panels [40–45].

Stringers are an efficient structural solution to increase the stiffness of the panels with a low increase of its total mass. Among the significative design factors, the bonding between skin and stiffener is one of the most critical aspects to consider, so an important number of studies has been devoted to analyse the behaviour of the interface stringer-panel [46–48]. Sometimes, the design requirements need that some stringers have a specific termination named run-out. A run-out is a cut-out with a certain angle at the end of the rib. These designs result in geometries with much more complex mechanical behaviour. For this reason, the behaviour of the stringer-panel interface, with a specific run-out termination, has been studied by different authors [49, 50].

Also, different types and geometries of run-out have been tested, either numerically [51–53] or experimentally [54, 55], and analysed to determine the advantages of the different designs. Other studies [56–60] compare the virtual and experimental tests regarding the damage behaviour.

In the present study the effect of different run-out geometric parameters in the behaviour of the panel-stringer specimen has been evaluated for four different run-out configurations. A virtual test has been carried out for each type using finite elements (FE) (Section 4.2). The interface stringer-panel has been analysed in detail with by means of cohesive elements. The analysis is focused in the damage of the interface (Section 3.3.1), the evolution of the crack (Section 3.3.1), the displacement of the panel (Section 3.3.2), the failure modes (Section 3.3.3) and the induced stresses (Section 3.3.4). During this analysis, numerical results are compared with an accurate experimental study performed by Greenhalgh and Garcia [54].

3.2 Virtual test

3.2.1 Specimen and test

In order to design a stringer run-out test a study carried out by Greenhalgh and Garcia [54] has been considered. These authors proposed three stringer run-out designs under tensile

loads and they analysed the behaviour until failure. The analysed specimen is a panel with a stringer run-out added in the longitudinal midplane (Fig. 3.1(a)). The shape of the clamp at the left side of Fig. 3.1(a) gives an extra stiffness to the run-out so it can be discarded from the analysis. This clamp avoids debonding in this run-out, which is forced to appear in the other run-out (right side of Fig. 3.1(a)). Therefore the debonding between the panel and the stringer can appear only in a specific location. Local displacement δ is applied at the tips of the specimen using the clamps.

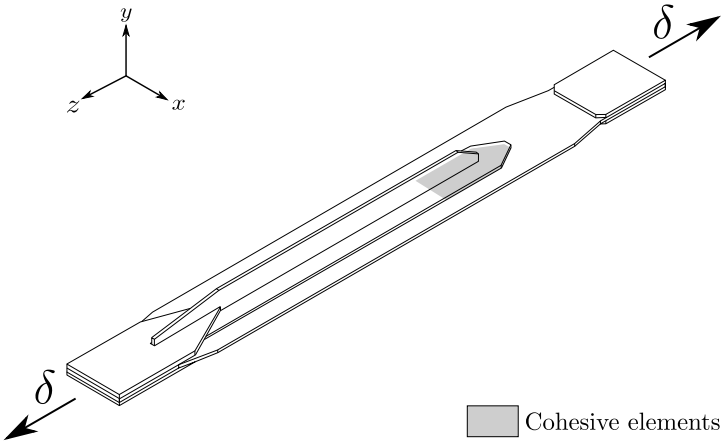

(a)

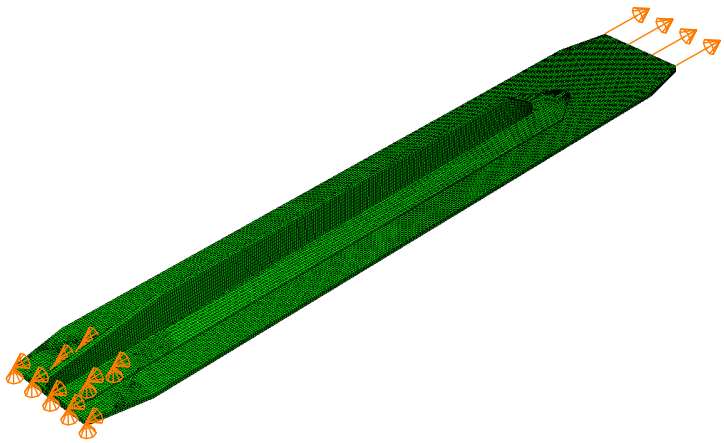

(b)

Figure 3.1: Schematic representation (a) and FE model (b) of the test.

In the modelling process, the square part of the clamps and the panel hold by them have been suppressed which to reduce the number of elements. Null displacement in all three direction are applied at the stiffened run-out clamp (left side of Fig. 3.1(b)) while $\delta_z = 3$ mm has been applied at the other tip (right side of Fig. 3.1(b)). The element type used is C3D8 (8-node linear brick three-dimensional solid element with full integration) of ABAQUS™

6.12-1 Standard [61] with a mean element edge length of 2 mm. Cohesive elements are used to simulate the behaviour of the adhesive in the longitudinal midplane of the panel-stringer set. For this reason, the mixed-mode improved cohesive elements proposed by Turon et al. [62] have been used to predict the initiation and evolution of debonding. These cohesive elements have been added at one end of the stringer (Fig. 3.1(a)) using a mean element edge length of 1mm.

β and d (Fig. 3.2) are two variables that define the different type of stringers. Each variable can take two values: $0°$ or $60°$ and 0 mm or 47 mm, respectively. Four types of stringer run-out (Fig. 3.2) are obtained by modifying these variables within these parameters: T1 ($\beta = 0°$; $d = 0$ mm), T2 ($\beta = 0°$; $d = 47$ mm), T3 ($\beta = 60°$; $d = 47$ mm) and T4 ($\beta = 60°$; $d = 0$ mm). In this study, these four different types of stringer run-out have been analysed and compared. Three of these types (T1, T2 and T3) have been studied by Greenhalgh and Garcia [54]. T4 has been defined by the authors of this study to analyse another possible design.

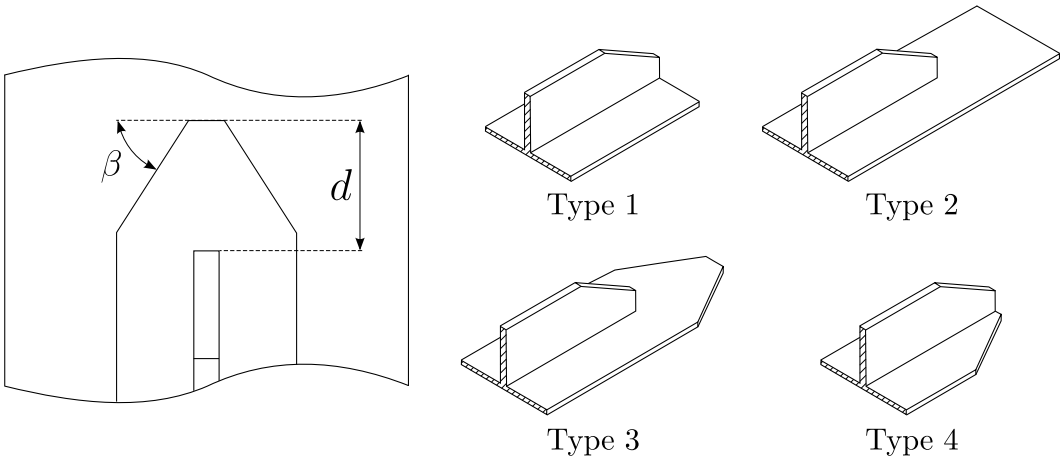

Figure 3.2: Design variables and types of stringer run-outs.

Stringer and panel are made of carbon fibre reinforced polymer AS4/8552. The properties of the material are given in a previous work [63]. Both components are bonded with adhesive FM-300K. The properties of this adhesive have been obtained experimentally with a Mixed-Mode Bending (MMB) test following ASTM D6671M-06 [64]. The tests have been carried out with mixed-mode ratios of 0%, 25%, 50%, 75% and 100%. The values of delamination initiation have been computed with the 5%/max method. These properties are shown in Table 3.1.

Property	Value	Units	Description
$\mathcal{G}_{\mathrm{I_C}}$	1.084	N/mm	Critical fracture energy in mode I.
$\mathcal{G}_{\mathrm{II_C}}$	4.931	N/mm	Critical fracture energy in mode II.
η	6.5687	-	Benzeggagh-Kenane interaction parameter between modes.

Table 3.1: FM-300K properties.

3.2.2 Simulation of panel-stringer debonding

The cohesive elements use the formulation of Benzeggagh and Kenane [65] to calculate the mixed mode fracture toughness, $\mathcal{G}_{\mathrm{C}}$.

$$\mathcal{G}_{\mathrm{C}} = \mathcal{G}_{\mathrm{I_C}} + (\mathcal{G}_{\mathrm{II_C}} - \mathcal{G}_{\mathrm{I_C}}) \cdot B^{\eta} \tag{3.1}$$

where B is the shear mode ratio calculated by:

$$B = \frac{\mathcal{G}_{\mathrm{II}} + \mathcal{G}_{\mathrm{III}}}{\mathcal{G}} \tag{3.2}$$

where $\mathcal{G}$ is the total fracture energy, calculated as $\mathcal{G}_{\mathrm{I}} + \mathcal{G}_{\mathrm{II}} + \mathcal{G}_{\mathrm{III}}$, where $\mathcal{G}_{\mathrm{I}}$, $\mathcal{G}_{\mathrm{II}}$ and $\mathcal{G}_{\mathrm{III}}$ are fracture energies in mode I, II and III respectively. Mode I is the opening mode, while mode II and III are the sliding shear and tearing modes, respectively.
The cohesive elements provide two output variables: the shear mode ratio (B) and the damage variable $\overline{r}$, which is defined as:

$$\overline{r} = \frac{\mathcal{G}_{\mathrm{d}}}{\mathcal{G}_{\mathrm{C}}} \tag{3.3}$$

where $\mathcal{G}_{\mathrm{d}}$ is the dissipated energy [62].
The variables analysed in this work are $\overline{r}$ (subsection 3.3.1) and B (subsection 3.3.3).

3.3 Results and Discussion

3.3.1 Damage

The results of the cohesive elements have been used to establish specimen failure to be compared with the experimental results of [54] and also to determine the evolution of

the damage. Greenhalgh and Garcia [54] define the failure as visual detection of stringer debonding. This method makes difficult to compare the experimental and virtual test results. Moreover, the objective of Greenhalgh and Garcia [54] is not the failure load, but the fracture mechanisms and failure processes. For this reason, the authors have defined a criterion to determine intervals of load in which failure takes place. These failure intervals are obtained by the calculation of the slope of the load-displacement graph and the observation of the progression of damage. This slope at load increment i has been calculated as:

$$K_i \simeq \frac{F_{i+1} - F_{i-1}}{\delta_{i+1} - \delta_{i-1}} \tag{3.4}$$

where F and δ are the applied force and displacement, respectively.

Once K of the set panel-stringer has been calculated it is possible to analyse the loss of stiffness during the virtual test (Fig. 3.3). When a sudden loss of the specimen stiffness is observed the onset of damage is considered to occur and the beginning of the failure interval is fixed. Then the visual observation of the results of the cohesive elements (3.4) is used to choose the end of the failure interval and verify its beginning. Both figures (Fig 3.3 and 3.4) number selected increments of the interval which relate them.

It is known that ply splitting appears in these specimens [54]. It is possible to introduce cohesive elements between the plies to simulate this splitting. But this possibility has been dismissed for the high increase of the computational cost and the consequent difficulty to obtain convergence. For these reasons, the results after the failure interval are not considered in the analysis.

In T1 and T2 (Fig. 3.3(a) and 3.3(b)), a large and fast loss of stiffness is observed. For this reason, the first few increments of the substantial negative slope have been selected as failure interval. On the other hand, T3 and T4 (Fig. 3.3(c) and 3.3(d)) have a progressive descendent slope. In addition, T3 has a strong fall after this progressive descendent slope. This strong fall indicates a important loss of stiffness and it permits to establish the end of failure interval at this point. However, it is difficult to determine the end of the interval for T4. In this case, the observation of the cohesive elements (Fig. 3.4(d)) is essential to determine when the crack long is enough to produce the failure. A similar crack length to T3 and T4 is chosen to determine the ending of the failure interval of T4. In the progress of damage in the cohesive elements (Fig. 3.4) it is observed that a bigger crack is needed to obtain an important loss of stiffness in T3 and T4. Moreover, the cohesive elements of T2 (Fig. 3.4(b)) do not converge. The fast propagation of the crack is a feasible reason of why this virtual model can not obtain results after 1.52 mm of applied displacement.

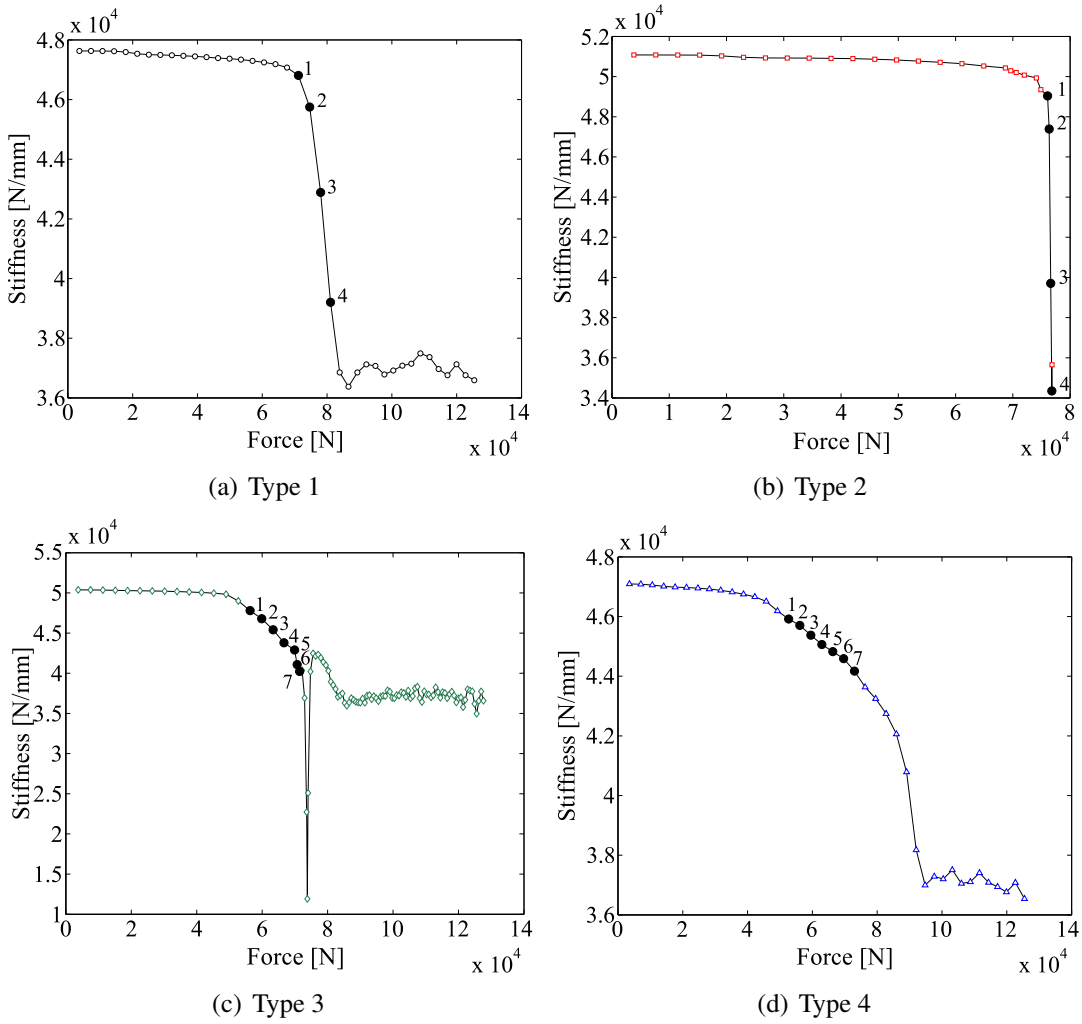

(a) Type 1 (b) Type 2

(c) Type 3 (d) Type 4

Figure 3.3: Stiffness vs. Force.

The intervals determined have been summarised and compared in Table 3.2. All intervals have similar order of magnitude although they have some differences. The properties of materials determined by the authors of this work, the usual errors and imperfections of an experimental test and the visual method used in the experimental tests are a feasible reason to obtain these differences. Furthermore, Greenhalgh and Garcia [54] determine an interval for T3 where they heard cracking noises and they report a failure load of 90kN. The experimental results of T1 and T3 lie within the intervals. T2 does not have the experimental results within the interval. But T2 have the biggest onset interval. Therefore, T2 is the most resistant run-out followed by T1, T3 and T4. These results agree with the experimental results.

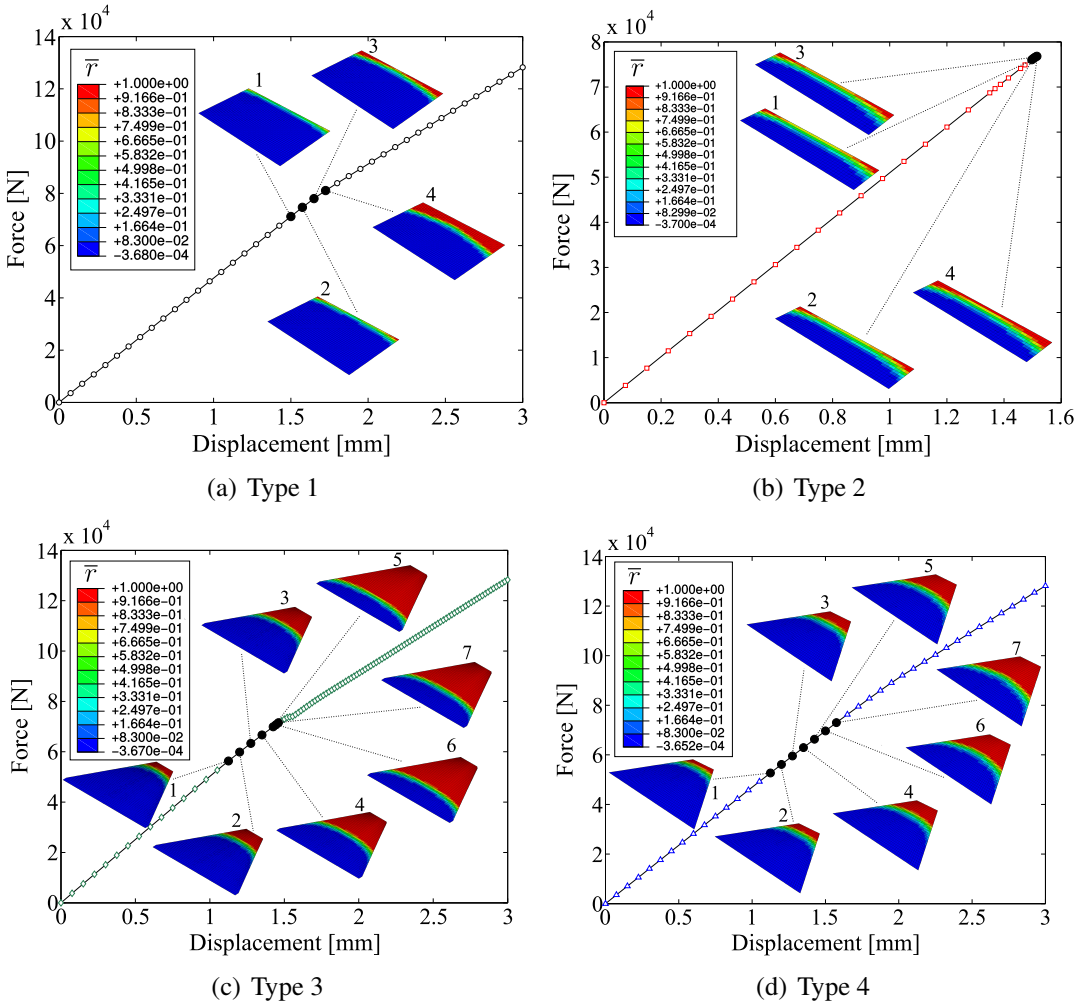

(a) Type 1 (b) Type 2

(c) Type 3 (d) Type 4

Figure 3.4: Force vs. Displacement.

Type	Virtual test results interval [kN]	Experimental results [kN]
1	71.15 - 81.08	73
2	76.06 - 76.82	83
3	56.32 - 71.45	52-62* (90)
4	52.68 - 72.98	-

* Interval at which Greenhalgh and Garcia [54] report cracking noises.

Table 3.2: Comparison with experimental results of [54].

Crack propagation

An analysis of the stability of the crack propagation has been carried out. Aircraft and aerospace structural design aims at damage tolerance, so stable crack propagation would be

a desired feature for any stiffener. Stability is determined by computing $\mathcal{G}/\mathcal{G}_C$ vs. the crack length a. Virtual Crack Closure Technique [66] and Eq. 4.3 are used to calculate $\mathcal{G}$ and $\mathcal{G}_C$, respectively. For this purpose, several FE models (without cohesive elements) with different crack length a in the midplane panel-stringer set have been computed.
The slope of the plot $\mathcal{G}/\mathcal{G}_C$ vs. a indicates the type of crack growth. Negative slope indicates stability, while a positive slope means unstable crack growth [67]. In Fig. 3.5 it is observed that all the considered types have an unstable crack growth but T3 and T4 have a negative slope and a plateau when $a \simeq 2$ mm, respectively. It is known [54] that ply splits occurs when $a \simeq 2$ mm and for this reason, numerical results after this point must be ignored. Considering this fact, the final conclusion is that all considered types have an unstable crack growth.

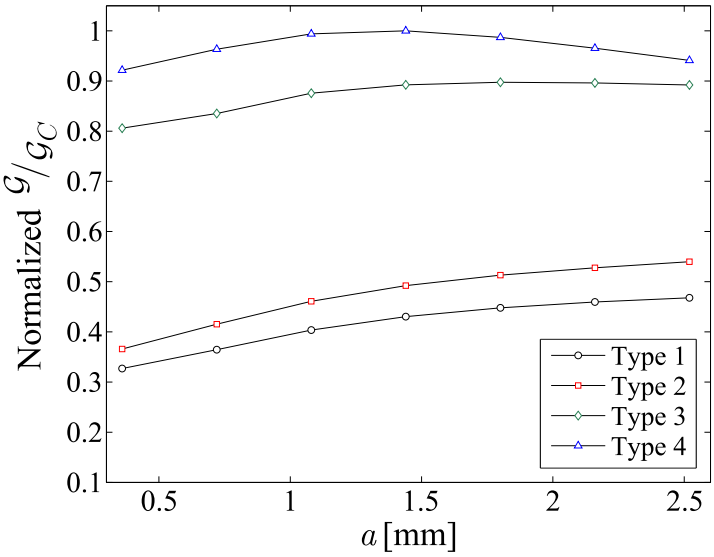

Figure 3.5: Normalized $\mathcal{G}/\mathcal{G}_C$ vs. crack length.

3.3.2 Displacements

The displacement that the panel is able to resist before the damage onset has been analysed. First it should be mentioned that, one of the particularities of the stringer run-out geometry is that a discontinuity in the stiffness is generated. This is due to the fact that the stringer rib provides a high stiffness but it stops at some point, where the global stiffness of the component drops drastically. When a tensile load is applied in a stiffened panel with a stringer run-out, the applied force generates a flexural moment caused by the different stiffnesses of the base and the stringer. Consequently, this flexural moment induces an out-of-plane (Y-axis) displacement. These displacements are analysed for each run-out type

and compared at the beginning of the failure interval (Fig. 3.6). T1 and T4 (Fig. 3.6(a) and 3.6(d)) show larger displacements (5.195 and 4.397 mm respectively) while T2 and T3 (Fig. 3.6(b) and 3.6(c)) have similar and smaller displacements (3.059 and 2.637 mm respectively).The maximum displacement is always located at the tip of the stringer run-out base. Stringer run-outs with longer base ($d = 47$ mm) show a nearly straight deformed shape after maximum displacement. This is due to the extra stiffness provided by the stinger base.

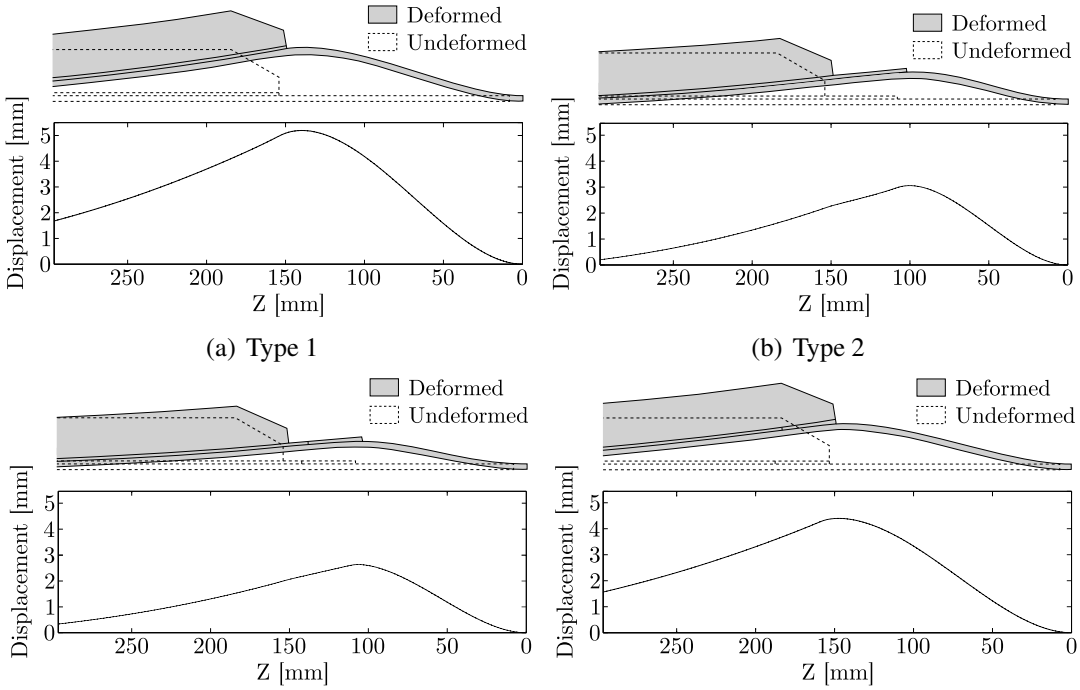

(a) Type 1 (b) Type 2

(c) Type 3 (d) Type 4

Figure 3.6: Displacements of the panel in Y-axis before failure.

3.3.3 Fracture modes analysis

The worst case for a stringer is a panel under tensile load [52] because the generated moment plus the in-plane load creates an important stress in mode II with the presence of mode I. For this reason, a study of the type of fracture mode that appears in the cohesive elements may be helpful for the design of stringers. Mode II is the most important mode that appears before the onset of damage in panels under tensile load [52, 54]. During the test, the shear mode ratio B progressively decreases and the cohesive element starts to damage. Therefore, more appearance of mode I will cause an earlier damage onset. Obviously, the apparition of a great presence of mode I makes the adhesive degradation greater since generally $\mathcal{G}_{\mathrm{II_C}} \gg \mathcal{G}_{\mathrm{I_C}}$ (e.g. see Table 3.1). Pure mode I only takes place when the cohesive element is completely

damaged. T1 and T2 have between 70-80% and 50-60% of B in the crack tip, while T3 and T4 have 30-40% and 30-45% respectively. One of the reasons why T3 and T4 have a lower failure load is the important presence of mode I before damage onse. In Fig. 3.7 the evolution of the mode change during de degradation of the cohesive elements is shown.

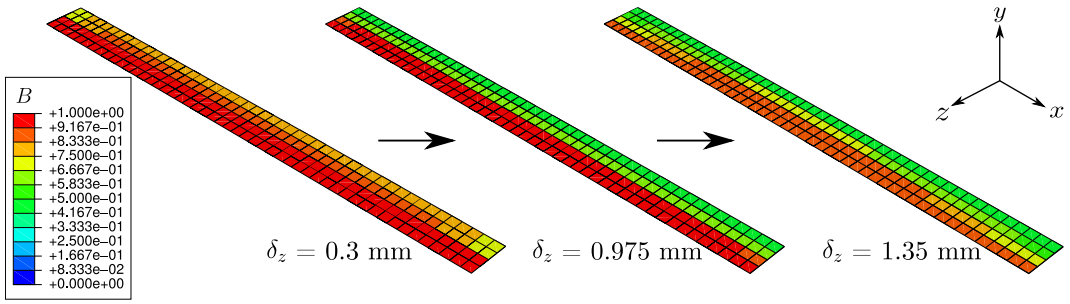

Figure 3.7: Evolution of shear mode ratio B in the crack tip of T2.

3.3.4 Stress analysis

Stress in Y-axis (σ_y) and stress in Y-plane in Z-direction (σ_{zy}) have been studied because they are the most important stresses that appear between panel and stringer. The tensional analysis is focused in the region of the stiffener tip, where high stress gradients appear at the connection between the skin and the stiffener. These stresses have been studied in the first increment of the failure interval, when the debonding starts.

The results obtained are summarized in Table 3.3. All types are observed to have similar σ_y with a maximum difference of 0.97%. This indicates that the geometry does not affect σ_y. On the other hand, σ_{zy} is influenced by the geometry. In the case of geometries in which stringer base has a 0° angle (T1 and T2), very similar results are observed, with only have a difference of 0.089%. On the other hand, the difference of 9.72% between T3 and T4 indicates that their tensions are also similar. Stringer bases with 60° angle tolerate a 31.48% less of σ_{zy} than stringer bases with 0° angles.

Type	σ_y [MPa]	σ_{zy} [MPa]
1	14.48	-55.69
2	14.44	-55.74
3	14.34	-36.22
4	14.34	-40.12

Table 3.3: Cohesive element stresses in the proximity of the crack tip.

σ_y and σ_{zy} always increase when we observe these tensions far of the base and crack tips. But T1 has some differences. This type has a reduction of the tensions in the rib zone.

3.4 Conclusions

An accurate study of four different type of stringer run-out has been presented. A virtual test of stiffened panel with stringer run-out under tensile load with cohesive elements in the interface stringer-panel has been carried out. This study has been realized in terms of damage and crack propagation, displacement of the panel in Y-axis, damage modes and tensions. The obtained results show that:

- Stringers with $\beta \simeq 0^\circ$ have a higher failure load.
- No studied stringer type have a stable crack growth.
- Stringer run-outs with long base ($d = 47$ mm) have smaller displacements of the panel in Y-axis than stringers run-out with short base ($d = 0$ mm).
- Shear mode presence is greater in stringer run-outs without angle in the base. This factor is directly proportional to the resistance to the damage. More mode I in the interface zone generates more degradation in the adhesive.
- σ_y is similar for all types of stringer. But σ_{zy} is higher in stringer bases without angles than those with angles.

Acknowledgments

The authors wish to acknowledge the Ministerio de Economía y Competitividad for the funding of the project DPI2009-08048 and particularly to Universitat de Girona for the research grant coded as BR2011/02.

Chapter 4

Damage tolerance optimization of composite stringer run-out under tensile load

This chapter contains the transcription of the submitted paper:

P. Badalló, D. Trias, E. Lindgaard. *Damage tolerance optimization of composite stringer run-out under tensile load*. Composite Structures.

Impact factor 3.120; Journal 2 of 24; 1st quartile; Category: Materials Science, Composites.

Abstract

Stringer run-outs are a common solution to achieve the necessary strength, stiffness and geometric requirements of some structural solutions. The mechanical behaviour and complexity of such design details requires careful and thorough studies to ensure the structural integrity of the structure. The influence of some geometric variables of the run-out in the interface of the set stringer-panel is crucial to avoid the onset and growth of delamination cracks. In this study, a damage tolerant design of a stringer run-out is achieved by a process of design optimization and surrogate modelling techniques. A parametric finite element model created with *python* was used to generate a number of different geometrical designs of the stringer run-out. The relevant information of these models was adjusted using Radial Basis Functions (RBF). Finally, the optimization problem was solved using Quasi-Newton method and Genetic Algorithms. In the solution process, the RBF were used to compute the objective function: ratio between the energy release rate and the critical energy release rate according to the Benzeggagh-Kenane mixed mode criterion. During the variable selection process, the stringer rib angle and the final run-out height were discarded, provided they have a low influence on the objective function. Conversely, the most significant geometric parameters are the base angle β and the distance between the rib tip and the stringer base tip (d). The optimal solution is found for the lowest possible values of β. If $\beta = 0^\circ$ could be used in the desing, $d = 0$ mm provides the optimal damage tolerance. In the other hand, if the specific design does not allow the use of $\beta = 0^\circ$, $d = 47$ mm provides the highest damage tolerance.

4.1 Introduction

The benefits of composite materials in aircraft/aerospace structures have been demonstrated in the last years. Stiffened panels are a common design strategy to obtain high stiffness in shell structures, keeping the lightness of the component and ensure the required buckling strength of the shell structure. As many others commonly used structural subcomponents these structures are frequently analysed [40–43] using the so-called virtual tests, which aims to reduce the design cost by reducing the number of test on real components.

One method to increase stiffness and buckling strength of shells is the use of stringers which are efficient but requires careful analysis and design of the panel-stringer interface [46–48]. Additionally, the geometric specification of the design sometimes requires a special termination of the stringer named run-out, which is a cut-out showing a certain angle at the tip. This termination can be classified to different types and geometries. Run-outs have been analysed by different authors [51–55] to define the behaviours and the best design. Hence, virtual tests, sometimes accompanied by experimental tests, have been deeply used to design and help to manufacture composite stringer run-outs [56–58, 60, 68].

However, the use of virtual tests needs large computation time for complex models. This prevents the use of optimization methods due to the necessity of generating a large number of different design cases (geometric, load states, boundary conditions, etc.) and their high computational cost. Metamodeling (or surrogate modeling) methods [69] are approximation techniques which can be used to substitute partially the solution of a complete finite element model. The use of surrogate models for design optimization or control of nonlinear systems has increased significantly in the last decade. The idea of surrogate models is to alleviate the burden of performing many computationally expensive analyses on a detailed model by constructing an approximation model (the surrogate model), that mimics the behaviour of the detailed simulation model as closely as possible while being computationally inexpensive to evaluate. Metamodeling may thus enable the use of design optimization techniques of complex and numerically expensive systems [70, 71].

In the present study, an optimization process with the aim of obtaining a damage tolerant design of run-out has been established and conducted. A parametric virtual test has been developed (Section 4.2) and Virtual Crack Closure Technique (VCCT) in the interface panel-stringer has been implemented. The structural influence of the different geometric variables of a run-out have been studied to choose the most significative ones (Section 4.3.1). The creation and verification of a Radial Basis Function (RBF) to reduce the computational time has been achieved (Section 4.3.4). Finally, optimizations of the RBF with Quasi-Newton method and Genetic Algorithms (GA) with different variable intervals have been performed

and compared (Section 4.4).

4.2 Virtual test

4.2.1 Specimen and test

The study carried out by Greenhalgh and Garcia [54] has been used to design the specimen and test. The specimen is a panel with an attached stringer run-out (also used in [72]). A displacement boundary condition δ is applied at the tip of the specimen (Fig. 4.1(a)). The stringer run-out of this model is defined by four variables: the stringer rib angle α, the stringer base angle β, the distance between the rib tip and the stringer base tip d, and the distance between the stringer base and the point where the stringer rib angle starts L_{ro} (Fig. 4.1(b)). In this study, *python* code together with ABAQUS$^{\text{TM}}$ 6.12-1 Standard [61] have been used to create a parametric model that automatically can be generated.

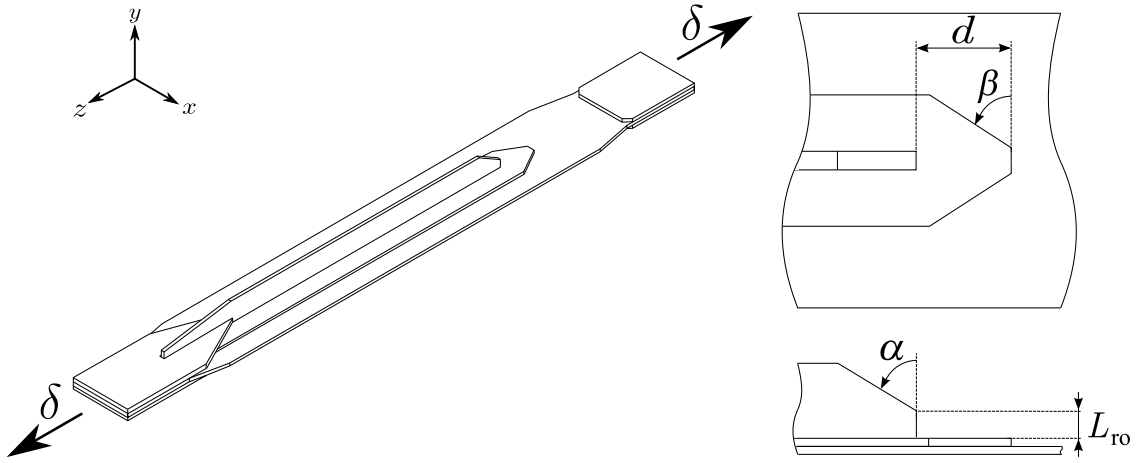

Figure 4.1: Schematic representation of the test and the initial design variables.

VCCT is used to determine the energy release rate of the existing initial crack (explained in Section 4.2.2). Previous work [72] shows that the formation of a crack always appears in the tip of the stringer base. For this reason, the initial crack is modelled in all the different cases at this location, in the longitudinal midplane between the stringer and the panel.

The material for both the stringer and the panel is AS4/8552 and they are bonded using FM-300K adhesive. All the material properties are described in Table 4.1.

Material	Property	Value	Units	Description
AS4/8552⋆	E_{xx}	135	GPa	Young's modulus in fiber direction.
	E_{yy}	9.6	GPa	Young's modulus in transversal fiber direction.
	E_{zz}	9.6	GPa	Estimated $E_{yy} = E_{zz}$. (transversally isotropic material).
	ν_{xy}	0.32	-	Poisson's modulus in XY plane.
	ν_{xz}	0.32	-	Estimated $\nu_{xy} = \nu_{xz}$. (transversally isotropic material).
	ν_{yz}	0.487	-	Poisson's modulus in YZ plane.
	G_{xy}	5.3	GPa	Shear modulus in XY plane.
	G_{xz}	5.3	GPa	Estimated $G_{xy} = G_{xz}$ (transversally isotropic material).
	G_{yz}	3.228	GPa	Shear modulus in YZ plane.
	X_T	2207	MPa	Longitudinal tensile strength.
	X_C	1531	MPa	Longitudinal compressive strength.
	Y_T	80.7	MPa	Transverse tensile strength.
	Y_C	199.8	MPa	Transverse compressive strength.
	$S_{L_{UD}}$	114.5	MPa	In-plane shear strength.
	$\mathcal{G}_{I_C}$ †	0.2839	N/mm	Critical fracture energy in mode I.
	$\mathcal{G}_{II_C}$ ‡	1.0985	N/mm	Critical fracture energy in mode II.
	ρ	$1.59 \cdot 10^{-9}$	T/mm^3	Density.
FM-300K	$\mathcal{G}_{I_C}$	1.084	N/mm	Critical fracture energy in mode I.
	$\mathcal{G}_{II_C}$	4.931	N/mm	Critical fracture energy in mode II.
	η	6.5687	-	Benzeggagh-Kenane interaction parameter between modes.

⋆ Source: [35]
† Source: [36]
‡ Source: [37]

Table 4.1: AS4/8552 and FM-300K properties.

Mesh

A comparative analysis was performed to determine the most appropriate element type. The elements compared have been C3D8 (8-node linear brick three-dimensional solid element), C3D8R (8-node linear brick three-dimensional solid element with reduced integration and hourglass control), C3D8I (8-node linear brick three-dimensional solid element with incompatible modes), C3D20 (20-node quadratic brick three-dimensional solid element) and SC8R (8-node, quadrilateral, first-order interpolation, stress/displacement continuum shell element with reduced integration). Solution time, reaction force and out-of-plane

displacement have been compared through mesh convergence studies (Table 4.2). All the element types have been compared with C3D20 element because it is well suited for bending problems. In our case, the computation time of SC8R element model is 100 times faster. The relative error is 0.14% and 1.69% in the reaction force and out-of-plane displacement, respectively. Therefore, SC8R element was chosen to mesh the whole model because it reduces the computational time and obtains reliable results.

Element type	Computation time [s]	Out-of-plane displacement [mm]	Reaction force [N]
C3D8	756	5.569	153 177
C3D8I	1445	5.062	153 629
C3D8R	161	5.694	152 961
C3D20	3402	5.135	153 064
C3D20R	1783	5.135	153 058
SC8R	34	5.048	153 271

Table 4.2: Results of comparative study of the element type.

The model has been partitioned in three parts (Fig. 4.2) to control all the element sizes of the mesh. These three parts are the stringer (without the crack zone), panel (without the crack zone) and the crack zone. All the parts have been bonded using TIE constraints (Fig. 4.2). The distance between the crack tip to the TIE zone has been analysed carefully to avoid interferences between the TIE constraint and VCCT (contact constraint in ABAQUS^{TM}).

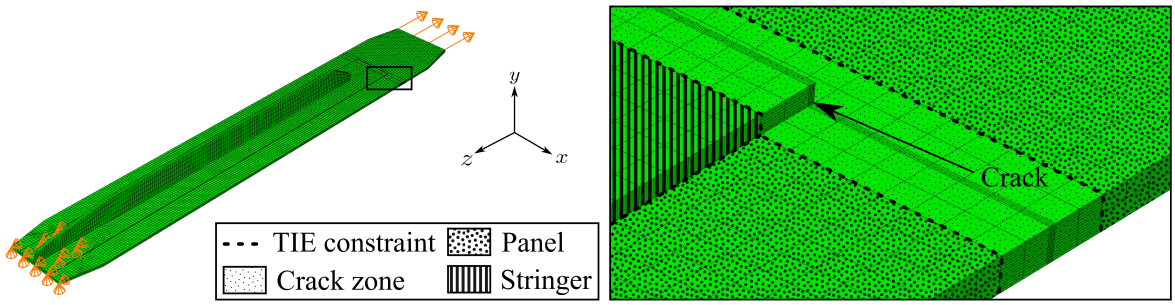

Figure 4.2: Details of the finite element model.

Krueger [66] proposes some guidelines about mesh size for the correct application of the VCCT (Section 4.2.2) in composite materials. The condition $0.1 \leq {}^{\triangle a}/_{h} \leq 1.0$ is achieved in our work to obtain acceptable results, where $\triangle a$ and h are the element length and the ply thickness respectively. In all the designed cases the mesh in the crack zone is controlled. Fig. 4.2 shows that the mesh in this zone is regular with the needed size to guarantee the correct computation of the VCCT.

4.2.2 Virtual Crack Closure Technique

VCCT [66] is used to calculate the energy release rate ($\mathcal{G}$). This technique assumes that the crack growth is self-similar. This means that if only the crack tip is observed, in the current step, the crack shape (displacements) and the reaction forces at the crack tip are assumed identical to those at the previous step.
The mixed mode fracture toughness, $\mathcal{G}_{\mathrm{C}}$, has been calculated with the formulation of Benzeggagh-Kenane [65].

$$\mathcal{G}_{\mathrm{C}} = \mathcal{G}_{\mathrm{I_C}} + (\mathcal{G}_{\mathrm{II_C}} - \mathcal{G}_{\mathrm{I_C}}) \cdot B^{\eta} \tag{4.1}$$

where $\mathcal{G}_{\mathrm{I_C}}$ and $\mathcal{G}_{\mathrm{II_C}}$ are the critical energy release rate in mode I (opening) and mode II (sliding), respectively. η is the Benzeggagh-Kenane interaction parameter between modes and B is the shear mode ratio calculated by:

$$B = \frac{\mathcal{G}_{\mathrm{II}} + \mathcal{G}_{\mathrm{III}}}{\mathcal{G}} \tag{4.2}$$

where $\mathcal{G}$ is the total energy release rate, calculated as $\mathcal{G}_{\mathrm{I}} + \mathcal{G}_{\mathrm{II}} + \mathcal{G}_{\mathrm{III}}$, and $\mathcal{G}_{\mathrm{I}}$, $\mathcal{G}_{\mathrm{II}}$ and $\mathcal{G}_{\mathrm{III}}$ are fracture energies in mode I, mode II and mode III (tearing), respectively.

4.3 Optimization

4.3.1 Design variables

The first model of the stringer run-out was defined with 4 parametric variables (Fig. 4.1): α, β, d and L_{ro}. In order to know if all these variables have a significant influence in the objective function, the analysis of variance test (ANOVA) [73] was used. The purpose of this test is to determine if the mean values of a group of data are significantly different to the values of another group of data. A group of data is significant when the probability (p-value) is less than a threshold (normally fixed between 0.05 and 0.01).
In our case, a group of 150 different design cases has been used to apply the ANOVA test. The results obtained are described in Table 4.3.
The obtained results (Table 4.3) indicate that α and L_{ro} are not significant for the value of the objective function. For this reason, only β and d have been selected as design variables for the optimization problem. The p-value computed for d is slightly greater than the threshold normally accepted. However, this value is significantly lower compared with α and L_{ro} . For this reason, d is accepted like an influential variable on the objective function.

Variable	p-value
α	0.6300
β	$2.5351 \cdot 10^{-10}$
d	0.0624
L_{ro}	0.6246

Table 4.3: Results of the ANOVA test.

4.3.2 Optimization problem

It is nowadays well-known that damage tolerant design in brittle and quasi-brittle materials like CFRP has to be based on fracture mechanical analysis, instead of using stress based criteria because of the difficulty of computing the stress field closes to the singularity (brittle materials) and at the failure process zone (quasi-brittle materials) [74]. For this reason, when looking for an optimal design in terms of damage tolerance, the objective function has to include some measure of the capacity of a crack to grow under the specified load. The failure index (Eq. 4.3) used as objective function in this study includes the current energy release rate normalized to the current critical energy release rate both depending on the current mode-mixity.

$$FI = \frac{\mathcal{G}}{\mathcal{G}_{\text{C}}} \tag{4.3}$$

The objective of the optimization problem is to minimize the FI, that is $FI(\beta, d)$. Stringer base angle β and the distance d between the rib tip and the stringer base tip are the two design variables, so the optimization problem is defined as:

$$\begin{aligned} &\text{Minimize} && FI(\beta, d) \\ &\text{Subject to} && 0 \leq \beta \leq 60 \\ & && 0 \leq d \leq 47 \end{aligned} \tag{4.4}$$

A Quasi-Newton method and a Genetic Algorithm (GA) [7] have been used to carry out the optimization. Quasi-Newton method is implemented in the function *fmincon* of the Optimization Toolbox™ of the commercial software MATLAB® [75]. A Non-dominate Sorting Genetic Algorithm II (NSGA-II) [33] is the variant used to achieve the optimization (implemented in the Optimization Toolbox™ of MATLAB®). In a previous work [63] NSGA-II was determined as one of the most effective algorithms.

4.3.3 Data sampling

The use of adequate "training" sample is crucial to obtain acceptable accuracy of the RBF (Section 4.3.4). For this reason, the correct distribution of the analysed cases has to be considered. In this study a Latin Hypercube Sampling (LHS) [76] has been used to guarantee the random, but uniform, distribution of points.

In our study the rate of change of the FI with respect to the design variables takes the largest values when $0 \leqslant \beta \leqslant 30$. Consequently, a more dense zone of points is established in this part of the design space (subregion 1, 2, 3 and 4 in Fig. 4.3). On the other hand, in order to capture the behaviour of the model in the extreme cases, a LHS has been used to distribute points in these specific regions. These points mark the limit of the design space with four "sets" of points, which are distributed in: $(\beta = 0) \wedge (0 \leqslant d \leqslant 47)$, $(\beta = 60) \wedge (0 \leqslant d \leqslant 47)$, $(d = 0) \wedge (0 \leqslant \beta \leqslant 60)$ and $(d = 47) \wedge (0 \leqslant \beta \leqslant 60)$. Finally, a sample of 400 points is created with all these cases (Fig. 4.3).

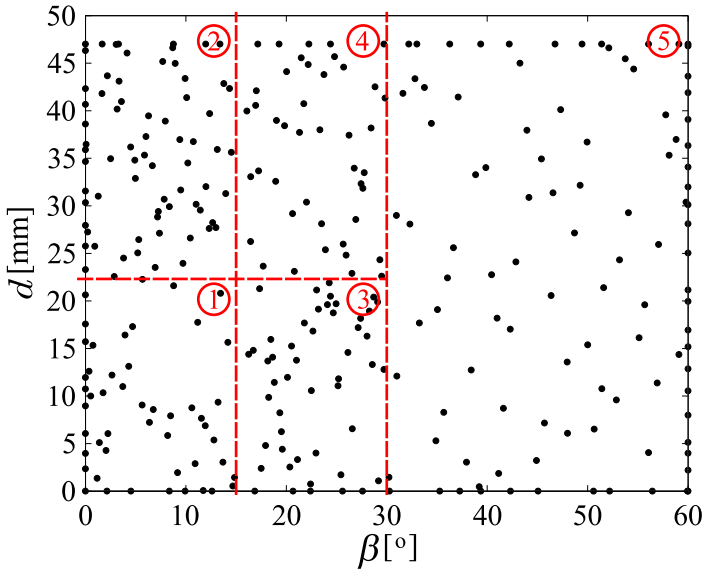

Figure 4.3: Initial data sampling.

4.3.4 Radial Basis Functions

The RBF [77] interpolation method constructs an approximation function ψ determining the coefficient c_0, c_1 and λ_i to generate a metamodel.

$$\psi = c_0 + c_1 x + \sum_{i=1}^{n} \lambda_i \varphi(\|x - x_i\|) \tag{4.5}$$

where n is the data sample size, φ is the radial function chosen, x_i is the observed input point and $\|\cdot\|$ is the Euclidean distance. In our case, we can define five different functions: Linear $\varphi = r$, cubic $\varphi = r^3$, thinplate $\varphi = r^2 \ln(r+1)$, gaussian $\varphi = \exp\left(-\frac{r^2}{2\phi^2}\right)$ and multiquadrics $\varphi = \sqrt{1+\frac{r^2}{\phi^2}}$. Where $r = \|x - x_i\|$ and ϕ is a constant close to the average distance between interpolation points. In addition, smoothing of the values of the RBF in the input points can be carried out to avoid possible input data noise. This smoothing does not force the RBF to obtain a result equal of a specific point of the input data. Thus, the smoothing value acts like the maximum absolute difference between the data point and the approximation provided by RBF. An example of the smoothing is shown in Fig. 4.4. An optimization with Quasi-Newton method to obtain the optimal smooth values for each radial basis function has been carried out. The smooth value is computed to obtain the minimum RMAE (Section 4.3.4).

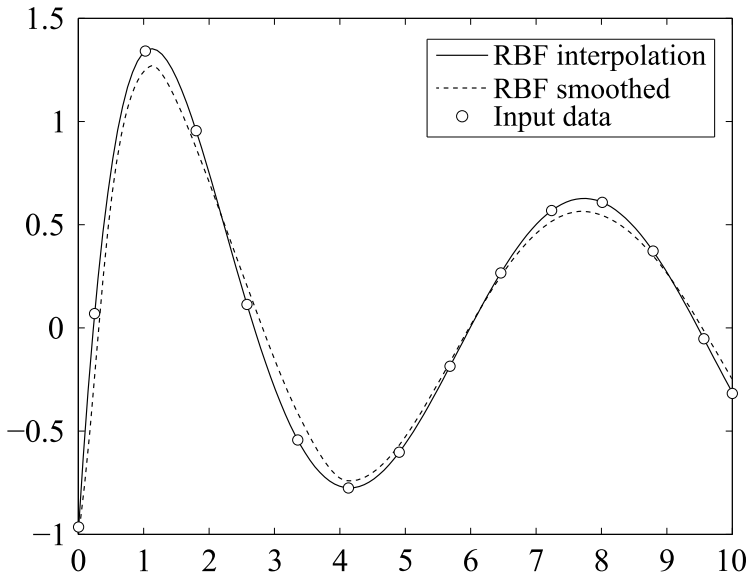

Figure 4.4: Exemple of smoothed RBF.

In order to reduce the total computational time of the optimization, the FE model has been replaced by the RBF. The automatic parametric model created with *python* and ABAQUS™ generates the "training" sample which is used to construct the RBF. Each model calculated by ABAQUS™ is a input point of the RBF.

Subregion

Sometimes a unique RBF cannot capture the global behaviour of the FE model. For this reason, it is necessary to divide the design space into subregions. Thus, the global RBF has been generated by five smaller RBF.
As a results of a non-linearity observed when $0 \leqslant \beta \leqslant 30$ the design space has been divided in four subregions in that zone. Only one subregion has been created when $30 < \beta \leqslant 60$ as a result of a correct behaviour of RBF in that subregion. It has been checked that the continuity across regions is acceptable. All the different subregions are numbered in Fig. 4.3.

Accuracy metrics

The accuracy of a metamodel is fundamental to obtain results close to the real case. According to [78, 79] cross-validation error is a common choice to measure the accuracy of the metamodel. In order to compare the different RBFs, a sample of confirmation points is needed. To obtain an acceptable result comparison, a large sample of confirmation points is generated. LHS is used to distribute 1000 points around the design space which are calculated with the FE model. These design points will be compared with the result of the same point predicted by the RBF. Two performance measures have been used to determine the accuracy of the different RBFs:

(a) Relative average absolute error (RAAE)

$$\text{RAAE} = \frac{\sum_{i=1}^{n} |y_i - \widehat{y}_i|}{n \cdot \text{STD}} \tag{4.6}$$

(b) Relative maximum absolute error (RMAE)

$$\text{RMAE} = \frac{\max\left(|y_1 - \widehat{y}_1|, |y_2 - \widehat{y}_2|, \ldots, |y_n - \widehat{y}_n|\right)}{\text{STD}} \tag{4.7}$$

where y_i is the FE value, $\widehat{y}_i$ is the value predicted by the RBF, n is the sample size and STD is the standard deviation of the "training" sample.

RAAE is an indicator of the global accuracy of the RBF. On the other hand, RMAE is more sensitive to error in a specific zone of the design space. Both errors indicate higher accuracy of the metamodel when their results decrease.

Verification of the RBF results

Once the different RBFs have been compared (and selected), a verification of the results obtained is needed. Thus, the sample of confirmation points created to obtain RAAE and RMAE has been used to compute the accuracy of the RBF. The mean of the relative error $\overline{\varepsilon_{\mathrm{r}}}$ and the standard deviation of the relative error $\sigma_{\varepsilon_{\mathrm{r}}}$ have been calculated to achieve a general overview of the accuracy of the RBF.

$$\overline{\varepsilon_{\mathrm{r}}} = \frac{\sum_{i=1}^{n} \varepsilon_{\mathrm{r}}}{n} \quad ; \quad \varepsilon_{\mathrm{r}} = \frac{|y_i - \widehat{y}_i|}{y_i} \tag{4.8}$$

where ε_{r} is the relative error.

4.4 Results and Discussion

The error of the subregions has been compared to determine the most accurate function to create the RBF. In our case, a total of ten different radial functions have been compared: the five function described above and their smoothings. RAAE and RMAE have been calculated for each radial basis function and their subregions. The most accurate results have been obtained by using linear smoothing (LS) and multiquadrics smoothing (MS). In an optimization process a reduced value of RMAE is desired, since a large local error in the fitting could lead to a wrong location of the optimal value. According to the results shown in Table 4.4, LS obtains a 1.07% lower than MS of the mean value of the subregions of RMAE. For this reason, LS has been selected to create the RBF to optimize the run-out.

Once the RBF has been chosen the $\overline{\varepsilon_{\mathrm{r}}}$ and $\sigma_{\varepsilon_{\mathrm{r}}}$ have been calculated. The obtained results are listed in Table 4.5. All the results of $\overline{\varepsilon_{\mathrm{r}}}$ are similar or smaller than 5%. This indicates a correct fit of the RBF and verifies that the RBF is suitable to use in an optimization process. At the same time, it was verified that the RBF and the finite element solution follow the same trend. Results also show that $\sigma_{\varepsilon_{\mathrm{r}}}$ is significant but indicates that 95% of the data (according $\overline{\varepsilon_{\mathrm{r}}} \pm 2\sigma_{\varepsilon_{\mathrm{r}}}$) have an absolute error less than 10%. Also, it is observed that the best results are obtained in subregion 5. This is a new indicator that in this subregion of the design space the variation (or noise) of the data is small and it helps to obtain a RBF more precisely.

Regarding computational time, each finite element model created needs about 1 minute considering re-meshing and solution. On the other hand, an evaluation of the RBF is achieved in about 0.005 seconds. Therefore, an optimization with RBF has been finished with about 1 second. Approximately 17 hours would have been required to carry out the optimization

Error type	RBF subregion	Linear smoothing	Multiquadrics smoothing
RAAE	1	0.3345	0.3037
	2	0.3650	0.3203
	3	0.6093	0.5803
	4	0.6342	0.6281
	5	0.2444	0.2163
RMAE	1	0.6812	0.6942
	2	0.7420	0.8228
	3	1.4112	1.3642
	4	1.5559	1.6625
	5	1.0094	0.9144

Table 4.4: Comparative error of RBF.

Linear smoothing		
RBF subregion	$\overline{\varepsilon_r}$ [%]	σ_{ε_r}
1	4.0970	2.2634
2	4.4413	2.5957
3	5.1949	2.6179
4	4.9158	3.0145
5	1.9518	1.8924

Table 4.5: Results of LS of the RBF.

with finite element models. The used computer is a HP Compaq dx2400 Microtower with an Intel® Core™ 2 Quad CPU Q8200 with 2.33GHz, 4GB of RAM with Ubuntu 14.04 LTS 64-bits and ABAQUS™ 6.12-1 Standard.

Two different types of problems have been solved. First, those problems in which β needs to be restricted to a short interval of values because of constructive reason and d may take any value between the global considered bounds (coded as BG). Next, problems in which d has to be restricted because of constructive reasons and β may take any value between $0°$ and $60°$ (coded as DG). Intervals of $10°$ of β for BG and intervals of 10 mm of d for DG are set (except the last one that is established in 7 mm, DG5 in Table 4.6). The optimization has been carried out with these different intervals and multiple results of FI have been obtained. Furthermore, the same intervals have been calculated by Quasi-Newton method and GA.

In table 4.6 the variables and results using Quasi-Newton method (β_{QN}, d_{QN} and FI_{QN}) and GA (β_{GA}, d_{GA} and FI_{GA}) are given. In BG problems, the optimal value of β is always the minimum value of the interval under consideration. Moreover, the optimal value of d_{QN} is

always 47 mm (except in the interval BG1 where a value close to 0 is obtained). On the other hand, d_{GA} gets different scattered values in general close to the lower bound of d. This is due to the fact that the objective function depends strongly on β and only slightly on d. Since the GA only performs evaluations of the objective function without computing gradients, the precision of the obtained solution is lower than that achieved with the Quasi-Newton method. With these specific results and observing FI_{GA} of BG we can conclude that the values of FI are similar for $d \simeq 0$ mm or $d = 47$ mm. However, in general, better results are achieved with $d = 47$ mm because we observed that FI_{GA} has a mean of difference of 5.86% higher than FI_{QN}. If DG is analysed we can observe that $\beta_{\text{QN}} = \beta_{\text{GA}} = 0°$ is the result obtained in all the cases for Quasi-Newton method and GAs. This behaviour certifies that the minimum value of β leads to a minimum outcome of FI . On the other hand, for those intervals under consideration where $d < 20$mm (DG1 and DG2), the optimal value of d corresponds to the lower bound of the interval. When considering d between 20 and 30 mm (DG3), the optimal value of d is found at an intermediate point of the interval. Finally, for $d > 30$mm (DG4 and DG5), the optimal value of d is always the upper bound of the interval under consideration. These intervals achieve the minimum result of FI with the maximum value of d . To understand this behaviour, in Fig. 4.5 the evolution of B respect to d when $\beta = 0°$ (DG cases) is shown, revealing that from a certain value of d (between 25 and 30 mm) the mixed mode ratio decreases substantially leading to a decrease of the failure index FI . In this moment, a minimum value of FI is obtained with a maximum value of d . In DG only a 0.07% of difference is obtained between the results of FI_{QN} and FI_{GA}.
The global optimum, without intervals, is $\beta = 0°; d = 5.85$ mm and $FI = 4.53$.

Code	β interval [°]	d interval [mm]	Quasi-Newton method			Genetic Algorithm		
			β_{QN} [°]	d_{QN} [mm]	FI_{QN}	β_{GA} [°]	d_{GA} [mm]	FI_{GA}
BG1	0-10	0-47	0	5.85	4.53	0	5.85	4.53
BG2	10-20		10	47	7.56	10	2.73	7.69
BG3	20-30		20	47	8.17	20	0.66	8.75
BG4	30-40		30	47	8.51	30	5.87	9.30
BG5	40-50		40	47	9.48	40	4.64	10.29
BG6	50-60		50	47	10.32	50	15.13	10.82
DG1	0-60	0-10	0	5.85	4.53	0	5.85	4.53
DG2		10-20	0	10	5.07	0	10	5.07
DG3		20-30	0	23.5	4.59	0	23.5	4.59
DG4		30-40	0	40	5.54	0	39.37	5.55
DG5		40-47	0	47	5.51	0	45.77	5.52

Table 4.6: Interval optimums.

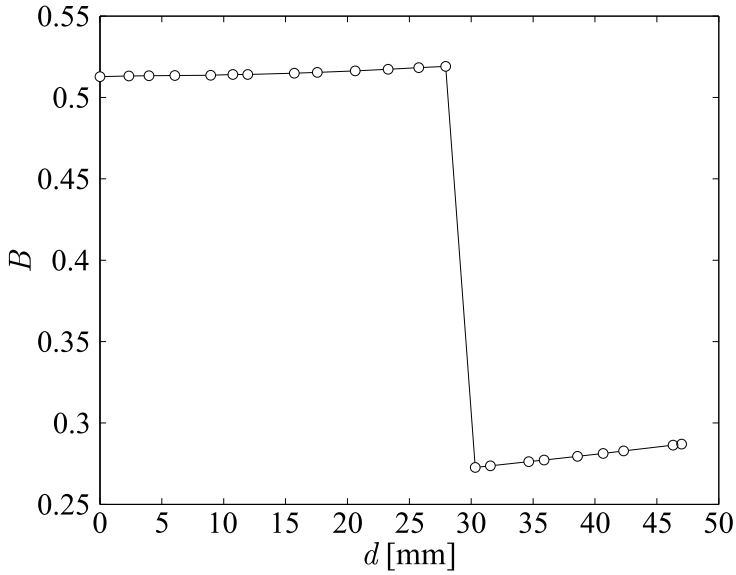

Figure 4.5: B vs. d when $\beta = 0°$.

Both ANOVA and optimization results show that the influence of the β in the results is clear. When $\beta = 0°$ the value of FI is the smallest. This is because the area in the stringer base edge (where the crack appears) decreases as β increases. This part of the stringer base resists and transmits all the tensile stress applied to the panel. For this reason, when this area increases the strength of the interaction panel-stringer increases accordingly. Then, the influence of d is not as significant as that of β .

In the previous work [72], more sophisticated finite element models were carried out. This model was solved in ABAQUS^{TM} 6.12-1 Standard in which mixed-mode improved cohesive elements [62] were added in the joint between the panel and the stringer to simulate the adhesive. All the results of the present work agree with the results computed in the previous work [72] and the experimental tests carried out by Greenhalgh and Garcia [54]. Both conclude that the stringer run-out with $\beta = 0°$ and $d = 47$ mm is the best design with the highest failure load. Furthermore in [72] it is determined that the second best design is achieved with $\beta = 0°$ and $d = 0$ mm. Therefore, the method used in the present work is reliable since it obtains the same results as experimental tests and finite element models with cohesive elements.

4.5 Conclusion

A process to design a damage tolerance optimization of composite stringer run-out under tensile load has been presented. A preliminary study of the design variables has been carried

out in order to determine the more influential ones in the opening of the crack between panel and stringer. Metamodelling in terms of Radial Basis Function (RBF) have been used to substitute the results of a finite element model. Moreover, the results of Quasi-Newton method and GA have been compared.
The proposed method involves some trial-and-error process to determine a RBF that properly fits the finite element model results. This process needs of a considerable amount of finite element models. On the contrary, when the RBF is created with an acceptable error, the computational time can be reduces considerably. The authors conclude that the proposed method permits the calculation of a composite material structure with reliability and reduce computational time, discarding some non-influential design variables.
The obtained results show that:

- α and L_{ro} have a very low influence on FI .
- β has an important contribution on FI . On the other hand, d has an influence but it is not relevant enough.
- To obtain better results of FI the lower possible value of β should be used. Regarding d, $d \simeq 0$ mm or $d \simeq 47$ mm could be used. Even though the FI are similar for $d \simeq 0$ mm and $d \simeq 47$ mm, the second ones gives slightly better results when $\beta \neq 0^{\circ}$.
- When $\beta \simeq 0^{\circ}$ and $d \simeq 0$ mm the optimum damage tolerance design is obtained.
- RBF is an acceptable metamodeling method which could be useful for similar optimization problems.
- The quality of the initial sampling is vital to create an accurate RBF.
- The optimization of the RBF carried out by Quasi-Newton method is faster and obtains better results than GAs.

Acknowledgments

The authors wish to acknowledge the Ministerio de Economía y Competitividad for the funding of the project MAT2013-46749-R and particularly to Universitat de Girona for the research grant coded as BR2011/02.

Chapter 5

Conclusions

The stiffened panels are a frequently used solution in the aircraft/aeronautical industry in the last decades. This type of panels are stiffened adding stringers which provide a minimum increase of weight. Often, the stringers need to have a specific shape for design and constructive reasons. For example, the run-out: a stringer with a cut-out with certain angle at the end of the rib. All these factors, together with the increment in the use of the composite materials, show the necessity of a deep analysis of this structural component. For this reason, this thesis is aimed to analyse and to optimize stringers with different computational techniques.

In Chapter 2 three different GAs have been compared in a multi-objective optimization of a simple stringer of composite material under compression load. A finite element model of a T-shape stringer is created with damage in the middle of the rib where a failure criterion is applied. When failure occurs the design is considered unfeasible and it is discarded. A preliminary study of the specimen has been used as a benchmark to demonstrate that the optimization process computes the optimal solution. The algorithms (AMGA, NCGA and NSGA-II) have been compared in terms of objective functions (F_{obj}), number of generations and computing time. A high and similar values of F_{obj} have been observed for AMGA and NSGA-II. On the other hand, NCGA and NSGA-II obtain a lower number of generations needed to arrive to the optimum, although AMGA only has a slightly higher value. Also, it is observed that computational time is a non-influential parameter for the comparison. This affirmation might be affected by the small number of variables used on this study because all the GA obtain a similar values of time. Therefore, different initiation modes for each GA have been used to know their influence on the result: Distributed population (DP), random (R) and initial solution (IS). Finally, AMGA and NSGA-II are selected as a most recommended GAs to use because they achieve a similar results.

Once different GAs have been analysed, a complex case of study is chosen and analysed: a stiffened panels with a stringer run-out under tensile load. In Chapter 3 this case is computed with finite elements in ABAQUS$^{\text{TM}}$ 6.12-1 Standard. The stringer run-out is added to the panel with mixed-mode improved cohesive elements. This study was achieved in terms of damage, crack propagation, out-of-plane displacement, fracture modes and stress analysis. The damage study was compared with the experimental results achieved by other authors to certificate the accuracy of the model. This comparative study concludes that the model carried out obtains similar results in terms of damage location and critical failure load. Then, all the finite element models conclude than these type of stringers have an unstable crack growth and that stringer with angle in the base shows lower shear fracture mode. This last factor affects directly to the damage tolerance because the higher presence of mode I in

the panel-stringer interface zone degrades the adhesive faster. On the other hand, the stress analysis reveals that similar σ_y for all types of stringer. In opposite, the stringers without angles in the base achieve higher σ_{zy}. Finally, two small guidelines are proposed: stringer without angle in the base ($\beta = 0°$) achieves a higher failure load and stringer run-outs with short base ($d = 0$ mm) exhibit a higher out-of-plane displacement.

Finally, in Chapter 4 a method to design a damage tolerance optimization is developed. A simplification of the virtual test presented in Chapter 3 is designed to reduce the computational time without a important loss of precision. Then, a preliminary study of the stringer variables has been performed to discard the less influential variables. Moreover, a failure index (FI) based on mixed-mode fracture energies is chosen as a objective function for the optimization problem. On the other hand, a metamodel with Radial Basis Function (RBF) is created. This metamodel is used to carry out the evaluation of the objective function instead of using a finite element model for that purpose, and so, a considerable reduction of the computational time is achieved. Different techniques to compute the accuracy and to verify the results of the various RBFs have been presented. Although the good results obtained, this method required a large number of iterations to fit properly the RBF. Also, the necessity to have a quality of the initial sampling to obtain a accurate RBF has been detected. Newly, some guidelines to design a tolerance damage run-out have been proposed. The low influence on the FI of the variables α and L_{ro} has been determined. On the contrary, β is the variable most influential and it leads to better results of FI with its lower possible value. Furthermore, FI is similar for $d \simeq 0$ mm and $d \simeq 47$ mm but the second one obtains lightly better results when $\beta \neq 0°$. Finally, the optimum damage tolerance design is given when $\beta \simeq 0°$ and $d \simeq 0$ mm.

After of this research work, the following future work is proposed:

- To design an optimization method which interacts with the RBF, so the approximation of the RBF can be improved only in those regions of space which are considered on the optimization process.
- To apply optimization techniques in a more complex structure, for example a stiffened panel with various stringer.
- To perform multi-objective optimization considering the mass of the component as a second objective.
- To create a complex virtual test to simulate the ply splits after the delamination of the stringer-panel set.

– To analyse the behaviour of the stringer run-out with different stringer shapes (I-shape, Z-shape, L-shape, hat, etc.).

– To carry out experimental test to check the virtual results.

Bibliography

[1] MIL-HDBK-17-3F. *Military Handbook, Polymer Matrix Composites*. U.S., Department of Defense, 2002.

[2] J. H. Holland. *Adaptation in natural and artificial systems: an introductory analysis with applications to biology, control, and artificial intelligence*. MIT Press, 1975.

[3] M. Dorigo and L. M. Gambardella. Ant colony system: A cooperative learning approach to the traveling salesman problem. *IEEE Transactions on Evolutionary Computation*, 1(1):53–66, 1997.

[4] J. Kennedy and R. Eberhart. Particle swarm optimization. In *IEEE International Conference on Neural Networks - Conference Proceedings*, volume 4, pages 1942–1948, 1995.

[5] R. Hooke and T. A. Jeeves. Direct search solution of numerical and statistical problems. *Journal of the ACM*, 8:212–229, 1961.

[6] K. Schittkowski. NLPQL: A fortran subroutine solving constrained nonlinear programming problems. *Annals of Operations Research*, 5(2):485–500, 1986.

[7] D. E. Goldberg. *Genetic Algorithm in search, optimization, and machine learnig*. Addison-Wesley publishing company, Inc., 1989.

[8] L. Lanzi and V. Giavotto. Post-buckling optimization of composite stiffened panels: Computations and experiments. *Composite Structures*, 73(2):208 – 220, 2006. ISSN 0263-8223.

[9] M. Corvino, L. Iuspa, A. Riccio, and F. Scaramuzzino. Weight and cost oriented multi-objective optimisation of impact damage resistant stiffened composite panels. *Computers & Structures*, 87(15-16):1033 – 1042, 2009. ISSN 0045-7949.

[10] M. Gigliotti, A. Riccio, L. Iuspa, F. Scaramuzzino, and L. Mormile. Weight optimisation of damage resistant composite panels with a posteriori cost evaluation. *Composite Structures*, 88(2):312 – 322, 2009. ISSN 0263-8223.

[11] A. Upadhyay and V. Kalyanaraman. Optimum design of fibre composite stiffened panels using genetic algorithms. *Engineering Optimization*, 33(2):201–220, 2000.

[12] F.-X. Irisarri, F. Laurin, F. H. Leroy, and J. F. Maire. Computational strategy for multiobjective optimization of composite stiffened panels. *Composite Structures*, 93 (3):1158–1167, 2 2011.

[13] O. Seresta, Z. Gürdal, D. B. Adams, and L. T. Watson. Optimal design of composite wing structures with blended laminates. *Composites Part B: Engineering*, 38(4):469–480, 6 2007.

[14] A. Todoroki and R. T. Haftka. Stacking sequence optimization by a genetic algorithm with a new recessive gene like repair strategy. *Composites Part B: Engineering*, 29(3): 277–285, 1998.

[15] L. Marín, D. Trias, P. Badalló, G. Rus, and J. A. Mayugo. Optimization of composite stiffened panels under mechanical and hygrothermal loads using neural networks and genetic algorithms. *Composite Structures*, 94(11):3321–3326, 11 2012.

[16] S. F. Badran, A. O. Nassef, and S. M. Metwalli. Y-stiffened panel multi-objective optimization using genetic algorithm. *Thin-Walled Structures*, 47(11):1331–1342, 11 2009.

[17] A. Puck and H. Schürmann. Failure analysis of FRP laminates by means of physically based phenomenological models. *Composites Science and Technology*, 58(7):1045–1067, 7 1998.

[18] C. G. Dávila, P. P. Camanho, and C. A. Rose. Failure criteria for FRP laminates. *Journal of Composite Materials*, 39(4):323–345, 2005.

[19] R. H. Lopez, M. A. Luersen, and E. S. Cursi. Optimization of laminated composites considering different failure criteria. *Composites Part B: Engineering*, 40(8):731–740, 12 2009.

[20] G. N. Naik, S. N. Omkar, D. Mudigere, and S. Gopalakrishnan. Nature inspired optimization techniques for the design optimization of laminated composite structures using failure criteria. *Expert Systems with Applications*, 38(3):2489–2499, 3 2011.

[21] G. N. Naik, S. Gopalakrishnan, and R. Ganguli. Design optimization of composites using genetic algorithms and failure mechanism based failure criterion. *Composite Structures*, 83(4):354–367, 6 2008.

[22] A. Konak, D. W. Coit, and A. E. Smith. Multi-objective optimization using genetic algorithms: A tutorial. *Reliability Engineering & System Safety*, 91(9):992–1007, 9 2006.

[23] E. Zitzler and L. Thiele. Multiobjective optimization using evolutionary algorithms - a comparative case study RID A-5738-2008. *Parallel Problem Solving from Nature - PPSN V*, 1498:292–301, 1998.

[24] E. Zitzler, K. Deb, and L. Thiele. Comparison of multiobjective evolutionary algorithms: empirical results. *Evolutionary computation*, 8(2):173–195, 2000.

[25] A. Gillet, P. Francescato, and P. Saffre. Single- and multi-objective optimization of composite structures: The influence of design variables. *Journal of Composite Materials*, 44(4):457–480, 2010.

[26] F. Wu, H. Zhou, J.-P. Zhao, and K.-F. Cen. A comparative study of the multi-objective optimization algorithms for coal-fired boilers. *Expert Systems with Applications*, 38(6): 7179–7185, 2011.

[27] T. Kunakote and S. Bureerat. Multi-objective topology optimization using evolutionary algorithms. *Engineering Optimization*, 43(5):541–557, 2011.

[28] S. Nagendra, D. Jestin, Z. Gürdal, R. T. Haftka, and L. T. Watson. Improved genetic algorithm for the design of stiffened composite panels. *Computers & Structures*, 58(3): 543–555, 2/3 1996.

[29] V. B. Gantovnik, Z. Gürdal, and L. T. Watson. A genetic algorithm with memory for optimal design of laminated sandwich composite panels. *Composite Structures*, 58(4): 513–520, 2002.

[30] *Isight 5.0 User's guide*. Dassault Systèmes Simulia Corp., Cary, North Carolina, USA, 2011.

[31] S. Tiwari, G. Fadel, P. Koch, and K. Deb. AMGA: An archive-based micro genetic algorithm for multi-objective optimization. In *Proceedings of the Genetic and Evolutionary Computation Conference, GECCO 2008*, pages 729–736, 2008.

[32] S. Watanabe, T. Hiroyasu, and M. Miki. Neighborhood cultivation genetic algorithm for multi-objective optimization problems. In *Proceedings of the Genetic and Evolutionary Computation Conference, GECCO 2002*, pages 458–465, 2002.

[33] K. Deb, A. Pratap, S. Agarwal, and T. Meyarivan. A fast and elitist multiobjective genetic algorithm: NSGA-II. *IEEE Transactions on Evolutionary Computation*, 6(2): 182–197, 2002.

[34] E. Zitzler, M. Laumanns, and L. Thiele. SPEA2: Improving the strength pareto evolutionary algorithm for multiobjective optimization. In *EUROGEN2001 Conference*, pages 95–100, 2001.

[35] C. S. Lopes, P. P. Camanho, Z. Gürdal, P. Maimí, and E. V. González. Low-velocity impact damage on dispersed stacking sequence laminates. Part II: Numerical simulations. *Composites Science and Technology*, 69(7-8):937–947, 2009.

[36] J. Renart, N. Blanco, E. Pajares, J. Costa, S. Lazcano, and G. Santacruz. Side clamped beam (SCB) hinge system for delamination tests in beam-type composite specimens. *Composites Science and Technology*, 71(8):1023–1029, 2011.

[37] J. Bonhomme, A. Argüelles, J. Viña, and I. Viña. Fractography and failure mechanisms in static mode I and mode II delamination testing of unidirectional carbon reinforced composites. *Polymer Testing*, 28(6):612–617, 2009.

[38] M. Crescenti. Post-buckling analysis of a carbon/epoxy stiffened panel pre-impacted on the stiffener edge. Master's thesis, Universitat de Girona, 2011.

[39] S. García, D. Molina, M. Lozano, and F. Herrera. A study on the use of non-parametric tests for analyzing the evolutionary algorithms' behaviour: A case study on the CEC'2005 special session on real parameter optimization. *Journal of Heuristics*, 15(6):617–644, 2009.

[40] R. Vescovini, C. G. Dávila, and C. Bisagni. Failure analysis of composite multi-stringer panels using simplified models. *Composites Part B: Engineering*, 45(1):939–951, 2 2013.

[41] R. Zimmermann, H. Klein, and A. Kling. Buckling and postbuckling of stringer stiffened fibre composite curved panels - Tests and computations. *Composite Structures*, 73(2):150–161, 5 2006.

[42] J. Bertolini, B. Castanié, J.-J. Barrau, and J.-P. Navarro. Multi-level experimental and numerical analysis of composite stiffener debonding. Part 1: Non-specific specimen level. *Composite Structures*, 90(4):381–391, 10 2009.

[43] J. Bertolini, B. Castanié, J.-J. Barrau, J.-P. Navarro, and C. Petiot. Multi-level experimental and numerical analysis of composite stiffener debonding. Part 2: Element and panel level. *Composite Structures*, 90(4):392–403, 10 2009.

[44] A. Riccio, A. Raimondo, and F. Scaramuzzino. A study on skin delaminations growth in stiffened composite panels by a novel numerical approach. *Applied Composite Materials*, 20(4):465–488, 2012.

[45] K. N. Anyfantis and N. G. Tsouvalis. Post buckling progressive failure analysis of composite laminated stiffened panels. *Applied Composite Materials*, 19(3-4):219–236, 2011.

[46] A. C. Orifici, S. A. Shah, I. Herszberg, A. Kotler, and T. Weller. Failure analysis in postbuckled composite T-sections. *Composite Structures*, 86(1-3):146–153, 11 2008.

[47] C. Meeks, E. Greenhalgh, and B. G. Falzon. Stiffener debonding mechanisms in post-buckled CFRP aerospace panels. *Composites Part A: Applied Science and Manufacturing*, 36(7):934–946, 7 2005.

[48] A. C. Orifici, R. S. Thomson, I. Herszberg, T. Weller, R. Degenhardt, and J. Bayandor. An analysis methodology for failure in postbuckling skin-stiffener interfaces. *Composite Structures*, 86(1-3):186–193, 11 2008.

[49] N. D. Flesher and C. T. Herakovich. Predicting delamination in composite structures. *Composites Science and Technology*, 66(6):745–754, 5 2006.

[50] Y. Volpert and T. Gottesman. Skin-stiffener interface stresses in tapered composite panel. *Composite Structures*, 33(1):1–6, 1995.

[51] A. Faggiani and B. G. Falzon. Numerical analysis of stiffener runout sections. *Applied Composite Materials*, 14(2):145–158, 2007.

[52] E. Cosentino and P. M. Weaver. Nonlinear analytical approach for preliminary sizing of discrete composite stringer terminations. *AIAA Journal*, 47(3):606–617, 2009.

[53] B. G. Falzon and D. Hitchings. The behavior of compressively loaded stiffener runout specimens - Part II: Finite element analysis. *Journal of Composite Materials*, 37(6): 481–501, 2003.

[54] E. Greenhalgh and M. H. Garcia. Fracture mechanisms and failure processes at stiffener run-outs in polymer matrix composite stiffened elements. *Composites Part A: Applied Science and Manufacturing*, 35(12):1447–1458, 12 2004.

[55] B. G. Falzon and G. A. O. Davies. The behavior of compressively loaded stiffener runout specimens - Part I: Experiments. *Journal of Composite Materials*, 37(5):381–400, 2003.

[56] B. G. Falzon, G. A. O. Davies, and E. Greenhalgh. Failure of thick-skinned stiffener runout sections loaded in uniaxial compression. *Composite Structures*, 53(2):223–233, 2001.

[57] J. Reinoso, A. Blázquez, A. Estefani, F. París, and J. Canas. A composite runout specimen subjected to tension-compression loading conditions: Experimental and global-local finite element analysis. *Composite Structures*, 101(0):274–289, 7 2013.

[58] S. Psarras, S. T. Pinho, and B. G. Falzon. Design of composite stiffener run-outs for damage tolerance. *Finite Elements in Analysis and Design*, 47(8):949–954, 8 2011.

[59] R. Krueger, J. G. Ratcliffe, and P. J. Minguet. Panel stiffener debonding analysis using a shell/3D modeling technique. *Composites Science and Technology*, 69(14):2352–2362, 11 2009.

[60] S. Psarras, S. T. Pinho, and B. G. Falzon. Investigating the use of compliant webs in the damage-tolerant design of stiffener run-outs. *Composites Part B: Engineering*, 45 (1):70–77, 2 2013.

[61] *Abaqus 6.12 User's manual*. Dassault Systèmes Simulia Corp., USA, 2012.

[62] A. Turon, P. P. Camanho, J. Costa, and J. Renart. Accurate simulation of delamination growth under mixed-mode loading using cohesive elements: Definition of interlaminar strengths and elastic stiffness. *Composite Structures*, 92(8):1857–1864, 7 2010.

[63] P. Badalló, D. Trias, L. Marín, and J. A. Mayugo. A comparative study of genetic algorithms for the multi-objective optimization of composite stringers under compression loads. *Composites Part B: Engineering*, 47(0):130–136, 4 2013.

[64] ASTM. Standard test method for mixed mode I - mode II interlaminar fracture toughness of unidirectional fiber reinforced polymer matrix composites ASTM D6671/D6671M-06. American Society for Testing and Materials, March 2006.

[65] M. L. Benzeggagh and M. Kenane. Measurement of mixed-mode delamination fracture toughness of unidirectional glass/epoxy composites with mixed-mode bending apparatus. *Composites Science and Technology*, 56(4):439–449, 1996.

[66] R. Krueger. The virtual crack closure technique: history, approach and applications. Technical report, NASA/CR-2002-211628, 2002.

[67] B. G. Falzon, D. Hitchings, and T. Besant. Fracture mechanics using a 3D composite element. *Composite Structures*, 45(1):29–39, 5 1999.

[68] R. Krueger and P. J. Minguet. Analysis of composite skin-stiffener debond specimens using a shell/3D modeling technique. *Composite Structures*, 81(1):41–59, 2007. ISSN 02638223.

[69] N. V. Queipo, R. T. Haftka, W. Shyy, T. Goel, R. Vaidyanathan, and P. K. Tucker. Surrogate-based analysis and optimization. *Progress in Aerospace Sciences*, 41(1): 1–28, January 2005. ISSN 03760421.

[70] R. Rikards, H. Abramovich, K. Kalnins, and J. Auzins. Surrogate modeling in design optimization of stiffened composite shells. *Composite Structures*, 73(2):244–251, May 2006. ISSN 02638223.

[71] N. Jansson, W. D. Wakeman, and J.-A. E. Månson. Optimization of hybrid thermoplastic composite structures using surrogate models and genetic algorithms. *Composite Structures*, 80(1):21–31, September 2007.

[72] P. Badalló, D. Trias, L. Marín, and Ll. Ripoll. Virtual test of different types of composite stringer run-outs under tensile load. Under review, 2015.

[73] G. E. P. Box, J. S. Hunter, and W. G. Hunter. *Statistics for Experimenters: Design, Innovation, and Discovery*. AMC, 2005.

[74] T. L. Anderson. *Fracture Mechanics: Fundamentals and Applications*. Taylor & Francis Group, 2005.

[75] *MATLAB Optimization Toolbox User's Guide*. The Math Works Inc, USA, 2014.

[76] M. D. Mckay, R. J. Beckman, and W. J. Conover. A comparison of three methods for selecting values of input variables in the analysis of output from a computer code. *Technometrics*, 42(1):55–61, 1979.

[77] N. Dyn, D. Levin, and S. Ripa. Numerical procedures for surface fitting of scattered data by radial functions. *Journal Scientific and Statistical Computing*, 7(2):639–659, 1986.

[78] R. Jin, W. Chen, and T. W. Simpson. Comparative studies of metamodelling techniques under multiple modelling criteria. *Structural and Multidisciplinary Optimization*, 23 (1):1–13, 2001.

[79] M. A. Nik, K. Fayazbakhsh, D. Pasini, and L. Lessard. A comparative study of metamodeling methods for the design optimization of variable stiffness composites. *Composite Structures*, 107:494–501, January 2014.

Appendix A

Published paper: A comparative study of genetic algorithms for the multi-objective optimization of composite stringers under compression loads

Composites: Part B 47 (2013) 130–136

Contents lists available at SciVerse ScienceDirect

Composites: Part B

journal homepage: www.elsevier.com/locate/compositesb

A comparative study of genetic algorithms for the multi-objective optimization of composite stringers under compression loads

P. Badalló *, D. Trias, L. Marín, J.A. Mayugo

AMADE, Dept. of Mechanical Engineering and Industrial Construction, Universitat de Girona, Campus Montilivi s/n, E-17071 Girona, Spain

ARTICLE INFO

Article history:
Received 9 May 2012
Received in revised form 4 September 2012
Accepted 12 October 2012
Available online 30 November 2012

Keywords:
A. Carbon fiber
C. Finite element analysis (FEA)
C. Numerical analysis
Genetic algorithm

ABSTRACT

Optimization methods are close to become a common task in the design process of many mechanical engineering fields, specially those related with the use of composite materials which offer the flexibility in the design of both the shape and the material properties and so, are very suitable to any optimization process. While nowadays there exist a large number of solution methods for optimization problems there is not much information about which method may be most reliable for a specific problem. Genetic algorithms have been presented as a family of methods which can handle most of engineering problems. However, starting from a common basic set of rules many algorithms which differ slightly from each other have been implemented even in commercial software packages. This work presents a comparative study of three common Genetic Algorithms: Archive-based Micro Genetic Algorithm (AMGA), Neighborhood Cultivation Genetic Algorithm (NCGA) and Non-dominate Sorting Genetic Algorithm II (NSGA-II) considering three different strategies for the initial population. Their performance in terms of solution, computational time and number of generations was compared. The benchmark problem was the optimization of a T-shaped stringer commonly used in CFRP stiffened panels. The objectives of the optimization were to minimize the mass and to maximize the critical buckling load. The comparative study reveals that NSGA-II and AMGA seem the most suitable algorithms for this kind of problem.

1. Introduction

The use of optimization methods in the design of structural components has been growing in the last years and becoming a usual step in the mechanical engineering workflow of many companies, specially those focused on aircraft/aerospace composite structures whose characteristics frequently meet the paradigm of a standard multiobjective optimization problem. For this reason, a large amount of optimization strategies ([1–5] among others) are available in the literature nowadays.

A structure of special interest which has been the object of optimization routines are composite panels stiffened with stringers. The optimization of the set panel-stringer is of high interest since this kind of structure is widely used in the aircraft industry. For them, Genetic Algorithms (GAs) [6], a family of evolutionary algorithms, have been successfully used, as reported in a large number of publications [7–11] among others. A case of special interest reported in the scientific literature is the optimization of the stacking sequence of composite laminates, for which GA have been used successfully [12,13]. However, in situations where the stacking sequence cannot be considered as a design variable but a imposed requirement, the minimization of the weight is achieved with geometrical parameters [14,15]. In that case, what makes different the optimization of composite structures from other materials is the use of failure mode based failure criteria such as Puck's [16] and LaRC [17]. These are in fact a set of failure criteria which assign a different index for the different failure modes under consideration. When they are included in optimization routines as non-smooth discontinuous constraints, the resulting optimization problem is very specific of composite materials, as can be concluded from some works analyzing the effect of different failure criteria in the optimal solution [18–20].

The original formulation of GAs is based on the concept of natural evolution: the survival of the fittest member, i.e., the better adapted members have more possibilities to transmit their characteristics to future generations. The translation of this strategy into an algorithm is performed by means of three operators:

- *Selection operator* which selects individuals with high fitness to form the mating pool.
- *Crossover operator* which permits the exchange of some characteristics between two or more members of the mating pool. Two individuals, called parents, exchange some characteristics to generate two new members, called children.

* Corresponding author.
E-mail addresses: pere.badallo@udg.edu (P. Badalló), dani.trias@udg.edu (D. Trias).

1359-8368/$ - see front matter © 2012 Elsevier Ltd. All rights reserved.
http://dx.doi.org/10.1016/j.compositesb.2012.10.037

- *Mutation operator* is implemented to save the process of losing genetic information during crossover. Random changes are applied in some individuals during the mutation process to preserve diversity in the population.

Although these three operators are the basis of a GA, there exist a large number of variations which implement different encodings, different selection operators, different methods for mating pairs or different strategies for mutation [21]. The behavior of a specific GA depends on the studied problem [22,23] and the design variables [24], for this reason, some previous experience or some comparative analysis is needed for selecting one GA out of a set of implemented GAs. Some comparative studies of evolutionary algorithms with different industrial cases have been already carried out [25,26], for example. These studies reveal that the best GA is different for each kind of problem.

A good choice when using GAs for the optimization of composite stiffened panels is a GA specifically designed for them, for example [27] and [28]. However, most of engineers are not familiar with the implementation of such algorithms and a commercial software with the most common GAs already implemented is a recommended option to carry out the optimization. In that case, a comparison of the most used GAs is a necessity for the choice as well.

The solution of the multi-objective optimization problem is linked to the concepts of dominance and non-dominance. When an individual is non-dominated it is a member of the Pareto's front, which is the set of possible optimal solutions. A candidate to solution **A** dominates candidate **B** if the conditions of Eq. (1) are fulfilled. On the other hand, if the Eq. (2) is satisfied **A** and **C** are considered non-dominated candidates.

$$f_i(\mathbf{A}) \prec f_i(\mathbf{B}) \leftrightarrow (f_1(\mathbf{A}) < f_1(\mathbf{B})) \wedge (f_2(\mathbf{A}) < f_2(\mathbf{B})) \quad (1)$$

$$f_i(\mathbf{A}) \sim f_i(\mathbf{C}) \leftrightarrow ((f_i(\mathbf{A}) \not\preccurlyeq f_i(\mathbf{C})) \wedge (f_i(\mathbf{A}) \not\succcurlyeq f_i(\mathbf{C})) \quad (2)$$

In this paper a comparative study of composite stringers under compression loads with three different GAs is carried out. The chosen three, implemented in software Isight™ [29], are: Archive-based Micro Genetic Algorithm (AMGA) [30], Neighborhood Cultivation Genetic Algorithm (NCGA) [31] and Non-dominate Sorting Genetic Algorithm II (NSGA-II) [32]. The main differences between these GAs are listed below:

- *NSGA-II*: After the creation of the parent population, sorting based on the non-dominance is used. A fitness (equal to non-domination level) is fixed in each solution. The best individuals of this ranking are used to create the new population using the selection, crossover and mutation operators.
- *AMGA*: This algorithm uses a small population size and creates an external archive with the best solutions obtained, which is updated every iteration. AMGA employs the concept of the non-dominance ranking of NSGA-II and it creates the parent population from the archive with the method of SPEA2 [33]. The mating pool is a derivation of the binary tournament selection method of NSGA-II. The use of the archive permits to obtain a large number of non-dominated points at the end of the simulation. AMGA is a GA highly based in NSGA-II.
- *NCGA*: A neighborhood crossover mechanism is added in the normal mechanisms of GAs which it improves the crossover operator. The pair of individuals to perform crossover is not randomly chosen, but the individuals who are close each other in the objective space are selected.

A T-shape stringer is used as a benchmark because of its simple geometry with only two design variables (Section 2.1) and because of its real-life interest in the design of stiffened panels. A preliminary study of the stringer is performed (Section 2.3) which permits to know the approximated optimal result. These structures are used for their compression behavior with low weight. For this reason, the objectives are both the maximization of the critical buckling load (P_{cr}) and the minimization of the stringer mass (m). In these cases, P_{cr} normally is most important for these structures and their design is in function of it. Then, in the optimization process is prioritized the P_{cr} than the mass (details in Section 3). Therefore, the previous optimal result is compared with the optimization results (Section 4) to know the reliability of the GA. Finally, a GA is proposed to use in the solution of similar multi-objective optimization problems.

2. Benchmark problem

2.1. Specimen

In this study a composite material T-shape stringer has been analyzed under compression load (Fig. 1). This geometry was selected since it provides both simplicity to run a benchmark and real life engineering interest.

The stringer is made from AS4/8552 pre-preg whose properties are described in Table 1. Stacking sequence is $[0/90/0_2/\pm45]$ for the stringer base and $[\pm45/0_2/90/0]_S$ for the stringer rib.

2.2. Virtual test

To carry out the optimization, a virtual test was modelled, using ABAQUS™ (Fig. 2). A compression load is applied on an end of the stringer and clamped by the other end. This compression load is applied by means of pottings, metallic elements where the stringer can be introduced and fixed with resin (Fig. 2). A potting only permits the displacement of the stringer base in X-axis and Y-axis in stringer rib. In the middle of the specimen a damaged zone was introduced to simulate the effects of an impact. This damaged zone is located in the stringer rib, in the middle of the specimen and it is modelled by reducing in a 50% the values of E_{xx} and X_C. The location of the damaged zone and the amount of properties reduction were obtained in a previous study [34]. It is added to simplify the finite element analysis (FEA) and to set the region where the first ply failure will appear. LaRC failure criteria is applied only in damaged zone to reduce computation time because it is known that the first ply failure will appear in the previously damaged zone. The elements used in mesh are S4 shell type (4-node shell element with full integration).

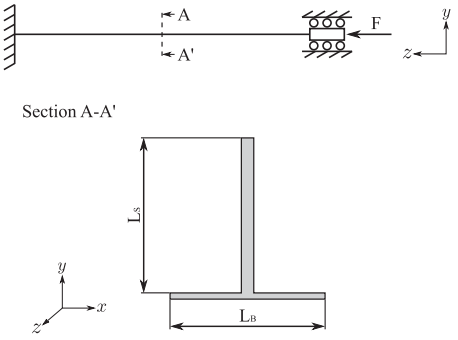

Fig. 1. Stringer section and schematic representation of the test.

Table 1
AS4/8552 properties. [36], unless otherwise stated.

Property	Value	Units	Description
E_{xx}	135	GPa	Young's modulus in fiber direction
E_{yy}	9.6	GPa	Young's modulus in transversal fiber direction
E_{zz}	9.6	GPa	Estimated $E_{yy} = E_{zz}$ (transversally isotropic material)
ν_{xy}	0.32	–	Poisson's modulus in XY plane
ν_{xz}	0.32	–	Estimated $\nu_{xy} = \nu_{xz}$ (transversally isotropic material)
ν_{yz}	0.487	–	Poisson's modulus in YZ plane
G_{xy}	5.3	GPa	Shear modulus in XY plane
G_{xz}	5.3	GPa	Estimated $G_{xy} = G_{xz}$ (transversally isotropic material)
G_{yz}	3.228	GPa	Shear modulus in YZ plane
X_T	2207	MPa	Longitudinal tensile strength
X_C	1531	MPa	Longitudinal compressive strength
Y_T	80.7	MPa	Transverse tensile strength
Y_C	199.8	MPa	Transverse compressive strength
S_{LT}	114.5	MPa	In-plane shear strength
G_{IC}[a]	0.2839	N/mm^2	Fracture energy toughness in mode I
G_{IIC}[b]	1.0985	N/mm^2	Fracture energy toughness in mode II
ρ	1.59×10^{-9}	T/mm^2	Density

[a] Source: [37].
[b] Source: [38].

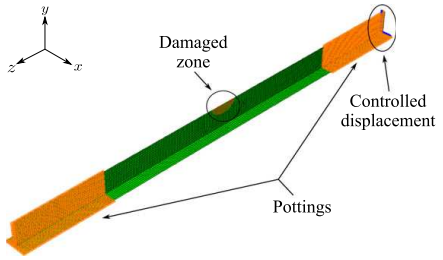

Fig. 2. Benchmark problem.

2.3. Preliminary study

A preliminary study aiming to determine the influence of design variables in the principal objective, P_{cr} and to obtain an approximated optimal solution was carried out. This results will be used to compare the performance of the analyzed algorithms.

Individuals with different dimensions of the stringer base length (L_B) and the stringer rib length (L_S) were distributed in design space and FEA was run for each individual. A design was considered unfeasible if the specimen damage started.

P_{cr} was calculated with the expression:

$$P_{cr} = RF \cdot \lambda \tag{3}$$

where RF is reaction force supported by the stringer and λ is the first stringer eigenvalue.

Once all distributed cases were executed the influence of each design variable was analyzed. As shown in Fig. 3 P_{cr} grows directly proportional to L_B until $L_B \simeq 29$ mm, when it starts to decrease. On the other hand, P_{cr} decreases inversely proportional to L_S (Fig. 4). This is because P_{cr} is dependent of λ, which is related to the vibration mode. At the same time, the vibration modes are dependent on the inertia. In our system of reference, the lowest inertia is I_{yy} and, for this reason, the specimen rotates respect to Y-axis. An increment of L_B generates an increment of I_{yy}, so the P_{cr} grows as well. When $L_B \simeq 29$ mm the vibration mode changes and λ decreases, and so does the P_{cr}.

When P_{cr} is plotted against L_B and L_S (Fig. 5) a peak is observed. This peak indicates the highest P_{cr}, that is the approximated optimal solution. This previous optimal solution has the values L_B approximately between 28 and 29 mm and L_S between 21 and 22 mm.

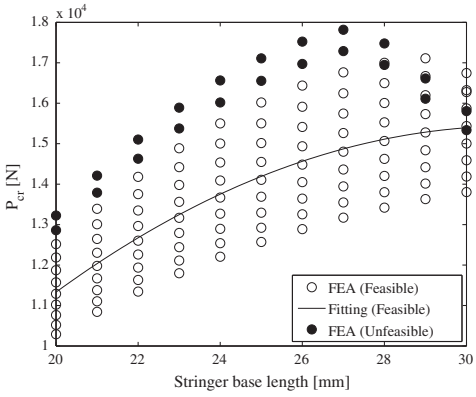

Fig. 3. P_{cr} vs. L_B.

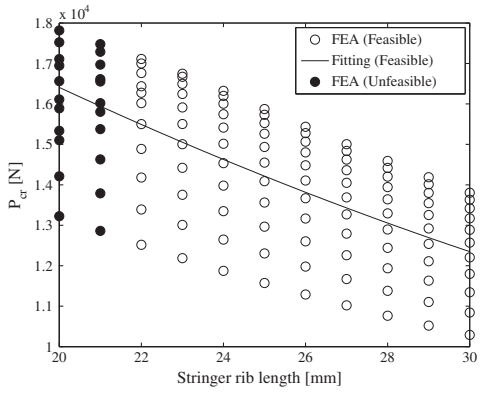

Fig. 4. P_{cr} vs. L_S.

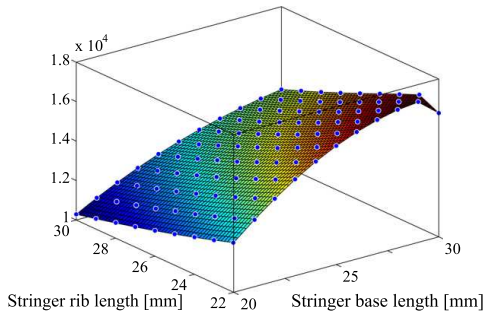

Fig. 5. P_{cr} vs. L_B and L_S.

3. Multi-objective optimization

The two objectives of the optimization problem are to maximize P_{cr} and to minimize m, that is $f_1(\mathbf{x}) = -P_{cr}$ and $f_2(\mathbf{x}) = m$. The design variables are the length of the base (L_B) and the rib (L_S) of the stringer.

The optimization problem is defined as:

$$\begin{aligned} &\text{Minimize} && F_{obj}(f_1(\mathbf{x}), f_2(\mathbf{x})) \\ &\text{Subject to} && g(\mathbf{x}) > 0 \\ &&& 20 \leqslant x_i \leqslant 30 \quad i = 1,2 \end{aligned} \tag{4}$$

where $\mathbf{x} = (L_B, L_S)$, $g(\mathbf{x}) = 1 - FI(\mathbf{x})$ and $FI(\mathbf{x})$ is the LaRC failure index.

Subsequently, the objective function (F_{obj}) is described:

$$F_{obj} = \sum \left(\frac{f_i(\mathbf{x}) \cdot w_i}{s_i} \right) \tag{5}$$

where $f_i(\mathbf{x})$ are the different objectives, w_i and s_i the weight and scale factors for each objective, respectively. To give priority to P_{cr} the values of the weights w_1 and w_2 are set 0.7 and 0.3, respectively.

The commercial software Isight™, with several optimization methods implemented, was used to solve the multi-objective optimization problem of Eq. (4). This software implements Eq. (5) which is used as a post-processing to extract the optimal solution from the Pareto front delivered by the GAs. Isight™ permits to link ABAQUS™ with the chosen optimization method and to calculate the P_{cr} for each individual. ABAQUS™ analyses the different geometries (individuals) computed for the optimization method. *RF*, λ, m and *FI*of the individuals are calculated by ABAQUS™ and P_{cr} by Isight™. Each GA has the same scheme. The used computer is a HP Compaq dx2400 Microtower with an Intel® Core™ 2 Quad

Table 2
Summary of obtained results.

GA	Initiation	Iteration	P_{cr} (kN)	m (g)	L_B (mm)	L_S (mm)	F_{obj}	Time (min)	Generations
AMGA	DP	1	17.386	65.24	28.49	21.37	67.36	580.8	14
		2	17.356	65.41	28.53	21.44	67.16	585.6	23
		3	17.340	65.54	28.58	21.49	67.04	597.5	23
		4	17.359	65.16	28.36	21.39	67.25	586.8	23
		5	17.335	65.25	28.36	21.45	67.09	590.7	22
	R	1	17.350	65.41	28.51	21.45	67.13	586.4	23
		2	17.394	65.19	28.47	21.35	67.41	575.6	23
		3	17.365	65.02	28.28	21.36	67.32	583.6	20
		4	17.385	65.26	28.51	21.38	67.35	584.2	20
		5	17.355	65.73	28.78	21.49	67.06	581.1	23
	IS	1	17.342	65.55	28.59	21.45	67.04	574.1	24
		2	17.362	65.31	28.48	21.42	67.22	582.9	22
		3	17.353	65.35	28.48	21.43	67.16	576.5	21
		4	17.386	65.28	28.52	21.38	67.35	584.0	19
		5	17.344	64.91	28.15	21.36	67.24	581.6	18
NCGA	DP	1	17.198	66.70	29.04	21.89	65.98	586.0	24
		2	16.948	68.08	29.34	22.50	64.31	596.3	22
		3	16.617	68.94	29.02	23.13	62.40	581.4	20
		4	16.877	67.55	28.75	22.50	64.12	577.9	20
		5	17.156	66.24	28.58	21.86	65.91	581.1	22
	R	1	17.103	65.01	27.66	21.66	66.02	568.7	16
		2	17.303	65.35	28.34	21.50	66.91	579.2	22
		3	17.313	65.38	28.39	21.49	66.95	581.8	22
		4	17.112	64.62	27.45	21.55	66.17	580.9	20
		5	17.303	65.14	28.20	21.46	66.97	577.2	18
NSGA-II	DP	1	17.364	65.23	28.42	21.40	67.25	578.1	23
		2	17.361	65.33	28.58	21.42	67.21	575.6	19
		3	17.322	65.09	28.22	21.42	67.08	587.9	21
		4	17.357	65.38	28.51	21.44	67.17	581.8	21
		5	17.319	64.98	28.13	21.41	67.09	588.9	20
	R	1	17.363	65.50	28.62	21.45	67.16	581.1	21
		2	17.375	65.05	28.32	21.35	67.36	577.7	16
		3	17.301	64.99	28.10	21.43	67.00	579.4	14
		4	17.372	65.41	28.58	21.42	67.24	580.7	17
		5	17.370	65.51	28.65	21.44	67.19	592.1	10
	IS	1	17.377	65.15	28.40	21.37	67.34	570.7	19
		2	17.394	65.44	28.58	21.44	67.19	580.1	21
		3	17.213	64.45	27.56	21.40	66.73	578.2	20
		4	17.151	64.19	27.29	21.40	66.49	563.7	22
		5	17.265	64.71	27.84	21.41	66.91	577.3	22

CPU Q8200 with 2.33 GHz, 4 GB of RAM, MS Windows XP Professional x64 Edition, Isight™ 5.5 and ABAQUS™ 6.9-3.

Once the optimization scheme was designed the different GAs were executed with different initiation modes. These modes set how the initial population is generated:

- *Distributed population* (DP): Equally spaced points in the design space are created.
- *Random* (R): A cloud of random cases is generated.
- *Initial solution* (IS): The starting initial population is a random cloud near to an initial geometry. For the analyzed case it was set L_B = 24 mm and L_S = 25 mm.

The GA parameters are fixed to analyse each GA with the same conditions. The values of parameters are listed below:

- *Number of generations*: 25.
- *Generation size*: 16 individuals.
- *Selection rate*: 50%.
- *Crossover probability*: 90%.
- *Mutation probability*: 50%.

These parameters generate 400 individuals for each GA and each initiation mode. AMGA is an exception, since it needs a different initial generation. For this reason, the value of initial population of AMGA is 40. This modification forces to change the number of generations to 24 to obtain the same approximated number of cases. On the other hand, Isight™ does not permit the IS mode with NCGA. Because of the fact that the GAs have a random component, related to crossover and mutation operators, each GA and each initiation mode was executed five times.

The executions for each GA and initiation mode are performed in random order to reduce the effect that other processes running in the computer might have on the results of the computational experiment.

4. Results and discussion

The comparison of the different algorithms is performed in terms of: obtained solution, computational time and number of generations to obtain the optimal. When an optimal individual does not improve after a specific generation, it is considered that this generation has reached the optimum.

The obtained results are listed in Table 2.

All values L_B and L_S of Table 2 are in agreement with the previous study, except four individuals. These four individuals, all in NCGA and DP mode (iterations 1, 2, 3 and 4), obtain a lower value of F_{obj} than the individuals of other GAs and initiation modes. A priori, this fact indicates that NCGA is the GA with the worst results, particularly with DP mode.

The mean, median and standard deviation were calculated for each GA and each variable (Table 3). This table shows that there are non-significant differences between the GAs for time variable, since the differences of mean are lower than 1%. Then, the mean of F_{obj} in NCGA is 2.44% and 2.26% lower than AMGA and NSGA-II respectively. Again, NCGA delivers different and lower results of the F_{obj}. However, AMGA and NSGA-II have a similar result with 0.18% of difference. NSGA-II achieves the best result of number of generations which is 9.91% lower than to AMGA, which occupies the second place. On the other hand, NCGA obtains a number of generations 2.83% lower than AMGA and 7.28% greater than NSGA-II.

To determine what statistical test is the most accurate to handle all data, the data type needs to be identified. The Kolmogorov–Smirnov test is used to determine the normality of the data (each GA and each initiation mode independently). This test concluded that all the sets of data are non-normal populations. In this situation, a non-parametric test is recommended. Furthermore, as reported in [35], non-parametric tests are specially useful for the analysis of evolutionary algorithms, in this case GAs. The Mann–Whitney U-test (also known as Wilcoxon rank sum test) was used to compare the data. The null hypothesis of the Mann–Whitney test is that compared populations have identical distributions with equal median, against the alternative of different medians. This test has to be applied by facing the data two by two which leads to face each GA to the others. This process was repeated in each comparison variable. The results of the Mann–Whitney test are in Table 4, where = is null hypothesis acceptance and $\neq$ is null hypothesis rejection.

Results of the test reflect that the time values are equal for all GA. Furthermore, an equal distribution is observed for F_{obj} in AMGA and NSGA-II, while different results are detected in NCGA. The lowest value of F_{obj} in NCGA (shown in Table 3) indicates that AMGA and NSGA-II are a good option to obtain a high and similar value of F_{obj}. On the other hand, an unequal distribution is obtained for the value of number of generations in AMGA and NSGA-II. Moreover, NCGA is similar to AMGA and NSGA-II. The values of Table 3 reveal that the number of generations for NCGA are approximately equidistant between AMGA and NSGA-II. For this reason, NCGA is similar to AMGA and NSGA-II but these are different among them. NSGA-II needs less generations to obtain the optimal. However, a high standard deviation indicates that a random component exists. Additionally, the initiation mode was studied. The distribution of the studied cases in each GA and each initiation mode was analyzed and the optimum evolution as well. The most representative cases are shown in Fig. 6.

Fig. 6a depicts the lines of distributed cases and the fact that the initial optimal solution is close to the final solution. This means that a DP mode enables the GA to achieve a faster optimal solution. On the other hand, a R mode has an expected random distribution (Fig. 6b). A possible remote initial optimal solution is the problem of a R mode, which may delay the arrival at the optimum. Finally,

Table 3
Statistics of the results.

Variable	GA	Mean	Median	Stand. dev.
F_{obj}	AMGA	67.21	67.22	0.13
	NCGA	65.57	66.00	1.50
	NSGA-II	67.09	67.17	0.23
Time	AMGA	583.4	583.6	5.9
	NCGA	581.0	581.0	6.9
	NSGA-II	579.6	579.4	6.9
Number of generations	AMGA	21.2	22	2.7
	NCGA	20.6	21	2.3
	NSGA-II	19.1	20	3.5

Table 4
Mann–Whitney test results.

	AMGA	NCGA	NSGA-II
F_{obj}			
AMGA		$\neq$	=
NCGA	$\neq$		$\neq$
NSGA-II	=	$\neq$	
Time			
AMGA		=	=
NCGA	=		=
NSGA-II	=	=	
Number of generations AMGA		=	$\neq$
NCGA	=		=
NSGA-II	$\neq$	=	

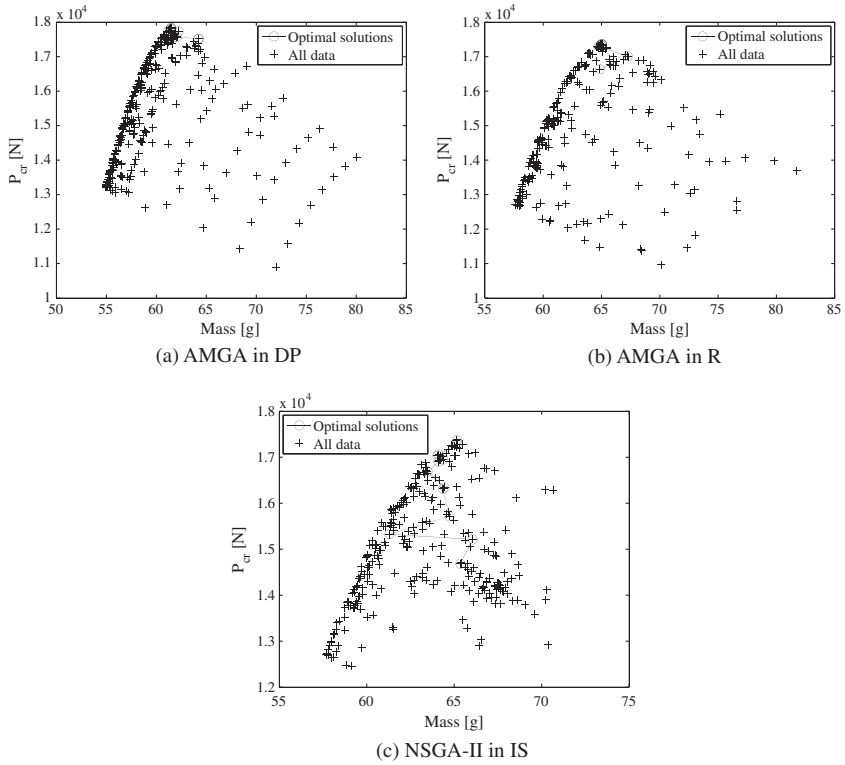

(a) AMGA in DP

(b) AMGA in R

(c) NSGA-II in IS

Fig. 6. Evolution of the optimums.

the first optimal solution is usually further from the final optimum in IS mode (Fig. 6c). This last initiation mode is recommended to improve a previous result.

5. Conclusion

A process to compare three GAs for the solution of multi-objective optimization problem of a simple composite material structure has been presented. A T-shape composite stringer under compression loads has been used as a benchmark for three different GA: AMGA, NCGA and NSGA-II. Moreover, a preliminary study of the specimen has been carried out to demonstrate that all the GAs reach the optimal solution.

An analysis of the results aids to recognize the first differences between the GAs. Therefore, a lower value of F_{obj} is observed in NCGA. A non-parametric test (Mann–Whitney U-test) has been used to compare the equality or inequality of the results. This test evidences that the computing time is independent on the GA used for the calculation because all the time values are similar. This conclusion might be affected by the use of a reduced number of design variables. On the other hand, both the AMGA and the NSGA-II achieve a high and similar value of F_{obj}. The lowest number of generations is obtained by NCGA and NSGA-II.

Finally, the different initiation mode (DP, R and IS) has been analyzed to appreciate the differences among them.

In conclusion, the results of F_{obj} and the number of generations indicate that the most recommended GAs for similar structural cases are NSGA-II and AMGA, because they give similar results.

Acknowledgments

The authors wish to acknowledge the Ministerio de Ciencia e Innovación for the funding of the Project DPI2009-08048 and particularly to Universitat de Girona for the research grant coded as BR2011/02.

References

[1] Holland JH. Adaptation in natural and artificial systems: an introductory analysis with applications to biology, control, and artificial intelligence. MIT Press; 1975.
[2] Dorigo M, Gambardella LM. Ant colony system: a cooperative learning approach to the traveling salesman problem. IEEE Trans Evol Comput 1997;1(1):53–66.
[3] Kennedy J, Eberhart R. Particle swarm optimization. In: IEEE International conference on neural networks – conference proceedings, vol. 4; 1995. p. 1942–8.
[4] Hooke R, Jeeves TA. Direct search solution of numerical and statistical problems. J ACM 1961;8:212–29.
[5] Schittkowski K. NLPQL: a fortran subroutine solving constrained nonlinear programming problems. Ann Oper Res 1986;5(2):485–500.
[6] Goldberg DE. Genetic algorithm in search, optimization, and machine learning. Addison-Wesley Publishing Company, Inc.; 1989.
[7] Lanzi L, Giavotto V. Post-buckling optimization of composite stiffened panels: computations and experiments. Compos Struct 2006;73(2):208–20.
[8] Corvino M, Iuspa L, Riccio A, Scaramuzzino F. Weight and cost oriented multi-objective optimisation of impact damage resistant stiffened composite panels. Comput Struct 2009;87(15–16):1033–42.
[9] Gigliotti M, Riccio A, Iuspa L, Scaramuzzino F, Mormile L. Weight optimisation of damage resistant composite panels with a posteriori cost evaluation. Compos Struct 2009;88(2):312–22.
[10] Upadhyay A, Kalyanaraman V. Optimum design of fibre composite stiffened panels using genetic algorithms. Eng Optimiz 2000;33(2):201–20.

[11] Irisarri FX, Laurin F, Leroy FH, Maire JF. Computational strategy for multiobjective optimization of composite stiffened panels. Compos Struct 2011;93(3):1158–67.
[12] Seresta O, Gürdal Z, Adams DB, Watson LT. Optimal design of composite wing structures with blended laminates. Compos Part B: Eng 2007;38(4):469–80.
[13] Todoroki A, Haftka RT. Stacking sequence optimization by a genetic algorithm with a new recessive gene like repair strategy. Compos Part B: Eng 1998;29(3):277–85.
[14] Marín L, Trias D, Badalló P, Rus G, Mayugo JA. Optimization of composite stiffened panels under mechanical and hygrothermal loads using neural networks and genetic algorithms. Compos Struct 2012;94(11):3321–6.
[15] Badran SF, Nassef AO, Metwalli SM. Y-stiffened panel multi-objective optimization using genetic algorithm. Thin-Wall Struct 2009;47(11):1331–42.
[16] Puck A, Schürmann H. Failure analysis of FRP laminates by means of physically based phenomenological models. Compos Sci Technol 1998;58(7):1045–67.
[17] Dávila CG, Camanho PP, Rose CA. Failure criteria for FRP laminates. J Compos Mater 2005;39(4):323–45.
[18] Lopez RH, Luersen MA, Cursi ES. Optimization of laminated composites considering different failure criteria. Compos Part B: Eng 2009;40(8):731–40.
[19] Naik GN, Omkar SN, Mudigere D, Gopalakrishnan S. Nature inspired optimization techniques for the design optimization of laminated composite structures using failure criteria. Expert Syst Appl 2011;38(3):2489–99.
[20] Naik GN, Gopalakrishnan S, Ganguli R. Design optimization of composites using genetic algorithms and failure mechanism based failure criterion. Compos Struct 2008;83(4):354–67.
[21] Konak A, Coit DW, Smith AE. Multi-objective optimization using genetic algorithms: a tutorial. Reliab Eng Syst Safety 2006;91(9):992–1007.
[22] Zitzler E, Thiele L. Multiobjective optimization using evolutionary algorithms – a comparative case study RID A-5738-2008. Parallel Prob Solving Nature – PPSN V 1998;1498:292–301.
[23] Zitzler E, Deb K, Thiele L. Comparison of multiobjective evolutionary algorithms: empirical results. Evol Comput 2000;8(2):173–95.
[24] Gillet A, Francescato P, Saffre P. Single- and multi-objective optimization of composite structures: the influence of design variables. J Compos Mater 2010;44(4):457–80.
[25] Wu F, Zhou H, Zhao JP, Cen KF. A comparative study of the multi-objective optimization algorithms for coal-fired boilers. Expert Syst Appl 2011;38(6):7179–85.
[26] Kunakote T, Bureerat S. Multi-objective topology optimization using evolutionary algorithms. Eng Optimiz 2011;43(5):541–57.
[27] Nagendra S, Jestin D, Gürdal Z, Haftka RT, Watson LT. Improved genetic algorithm for the design of stiffened composite panels. Comput Struct 1996;58(3):543–55.
[28] Gantovnik VB, Gürdal Z, Watson LT. A genetic algorithm with memory for optimal design of laminated sandwich composite panels. Compos Struct 2002;58(4):513–20.
[29] Isight 5.0 User's guide. Dassault Systèmes Simulia Corp. Cary, North Carolina, USA; 2011.
[30] Tiwari S, Fadel G, Koch P, Deb K. AMGA: an archive-based micro genetic algorithm for multi-objective optimization. In: Proceedings of the genetic and evolutionary computation conference, GECCO 2008; 2008. p. 729–36.
[31] Watanabe S, Hiroyasu T, Miki M. Neighborhood cultivation genetic algorithm for multi-objective optimization problems. In: Proceedings of the genetic and evolutionary computation conference, GECCO 2002; 2002. p. 458–65.
[32] Deb K, Pratap A, Agarwal S, Meyarivan T. A fast and elitist multiobjective genetic algorithm: NSGA-II. IEEE Trans Evol Comput 2002;6(2):182–97.
[33] Zitzler E, Laumanns M, Thiele L. SPEA2: improving the strength pareto evolutionary algorithm for multiobjective optimization. In: EUROGEN2001 conference; 2001. p. 95–100.
[34] Crescenti M. Post-buckling analysis of a carbon/epoxy stiffened panel pre-impacted on the stiffener edge. Master's thesis. Universitat de Girona; 2011.
[35] García S, Molina D, Lozano M, Herrera F. A study on the use of non-parametric tests for analyzing the evolutionary algorithms' behaviour: a case study on the CEC'2005 special session on real parameter optimization. J Heuristics 2009;15(6):617–44.
[36] Lopes CS, Camanho PP, Gürdal Z, Maimí P, González EV. Low-velocity impact damage on dispersed stacking sequence laminates. Part II: numerical simulations. Compos Sci Technol 2009;69(7–8):937–47.
[37] Renart J, Blanco N, Pajares E, Costa J, Lazcano S, Santacruz G. Side clamped beam (SCB) hinge system for delamination tests in beam-type composite specimens. Compos Sci Technol 2011;71(8):1023–9.
[38] Bonhomme J, Argüelles A, Viña J, Viña I. Fractography and failure mechanisms in static mode I and mode II delamination testing of unidirectional carbon reinforced composites. Polym Test 2009;28(6):612–7.

AMADE

ANÀLISI i MATERIALS AVANÇATS PER AL DISSENY ESTRUCTURAL